Col KEEL

AEDC-TR-71-105

TESTS CONDUCTED IN THE AEDC 16-FT TRANSONIC TUNNEL ON A 0.0226-SCALE MODEL OF THE C-5A AIRCRAFT FOR DATA CORRELATION BETWEEN THREE TRANSONIC WIND TUNNELS

J. A. Black
ARO, Inc.

July 1971

PROPULSION WIND TUNNEL FACILITY
ARNOLD ENGINEERING DEVELOPMENT CENTER
AIR FORCE SYSTEMS COMMAND
ARNOLD AIR FORCE STATION, TENNESSEE

NOTICES

When U. S. Government drawings specifications, or other data are used for any purpose other than a definitely related Government procurement operation, the Government thereby incurs no responsibility nor any obligation whatsoever, and the fact that the Government may have formulated, furnished, or in any way supplied the said drawings, specifications, or other data, is not to be regarded by implication or otherwise, or in any manner licensing the holder or any other person or corporation, or conveying any rights or permission to manufacture, use, or sell any patented invention that may in any way be related thereto.

Qualified users may obtain copies of this report from the Defense Documentation Center.

References to named commercial products in this report are not to be considered in any sense as an endorsement of the product by the United States Air Force or the Government.

TESTS CONDUCTED IN THE AEDC 16-FT TRANSONIC TUNNEL ON A 0.0226-SCALE MODEL OF THE C-5A AIRCRAFT FOR DATA CORRELATION BETWEEN THREE TRANSONIC WIND TUNNELS

J. A. Black
ARO, Inc.

FOREWORD

The experimental investigation reported herein was done at the request of the Air Force Flight Dynamics Laboratory (AFFDL), Air Force Systems Command (AFSC), and the Aeronautical Systems Division (ASD), AFSC, under Program Element 62201F, Project 1366.

The test data were obtained by ARO, Inc. (a subsidiary of Sverdrup & Parcel and Associates, Inc.), contract operator of the Arnold Engineering Development Center (AEDC), AFSC, Arnold Air Force Station, Tennessee, under Contract F40600-72-C-0003. A correlation investigation was conducted in three major facilities. The Propulsion Wind Tunnel (16T) phase was conducted by ARO, Inc., at AEDC in the periods December 30 and 31, 1969, and January 8 to 20, 1970, under ARO Project No. PB0068. The Cornell 8 by 8 Foot Wind Tunnel phase was conducted from April 8 through 10, 1970, and the NASA Ames 11-Foot Transonic Wind Tunnel phase was conducted from May 27 through June 10, 1970, and September 2 through 15, 1970. The correlation analysis of the data from the three facilities was completed in February 1971. The manuscript for this report which contains the PWT portion of the correlation data was submitted for publication on April 1, 1971.

This technical report has been reviewed and is approved.

George F. Garey
Lt Col, USAF
AF Representative, PWT
Directorate of Test

Joseph R. Henry
Colonel, USAF
Director of Test

ABSTRACT

Tests were conducted in the Propulsion Wind Tunnel (16T) on two configurations of a 0.0226-scale model of the C-5A aircraft for the purpose of data correlation with other major transonic test facilities. The results reported herein were obtained at Mach numbers from 0.600 to 0.825 and Reynolds numbers from 2.1 million to 4.2 million and represent the AEDC contribution to the correlation study.

CONTENTS

APPENDIX
ILLUSTRATIONS

Figure

Figure Page

NOMENCLATURE

C_A	Axial-force coefficient corrected for base axial-force effects, axial force/$q_\infty S$
C_D	Drag coefficient corrected for base drag effects, drag/$q_\infty S$
$\Delta C_{D_{Buoyancy}}$	Drag correction for effects of test section static pressure gradient
C_{D_b}	Base drag coefficient, base drag/$q_\infty S$
C_L	Lift coefficient, lift/$q_\infty S$
C_{L_o}	Lift coefficient at $\alpha = 0$
C_{L_α}	Rate of change of lift coefficient with angle of attack, per deg
C_m	Pitching-moment coefficient, pitching moment/$q_\infty S\bar{c}$, moments referenced to a fuselage station 26.786 in. aft of the model nose (see Fig. 2)
C_N	Normal-force coefficient, normal force/$q_\infty S$
$\bar{c}$	Wing reference chord, 0.699 ft
M_∞	Free-stream Mach number
ΔM_∞	Incremental Mach number correction
q_∞	Free-stream dynamic pressure, psf
Re	Reynolds number based on the wing reference chord, $V_\infty \bar{c}/\nu_\infty$
S	Wing reference area, 3.174 ft^2
V_∞	Free-stream velocity, ft/sec
W. L.	Model waterline, in.

α	Balance angle of attack, deg
α_{L_0}	Angle of attack at zero lift, deg
ν_∞	Free-stream kinematic viscosity, ft^2/sec

MODEL NOMENCLATURE (see Fig. 2)

B^{22}	Fuselage	Wing-Fuselage Configuration (WF)	Wing-Fuselage-Tail Configuration (WFT)
W^{12}	Wing		
Z^{f9}	Flap track fairings		
Z^{G27}	Nose landing gear fairing		
Z^{G28}	Main landing gear fairing		
Z^{W27}	Wing fillet		
b^{16}	Bullet		
D^8	Dorsal fin		
H^8	Horizontal stabilizer		
V^9	Vertical stabilizer		

SECTION I
INTRODUCTION

In 1967, after the basic wind tunnel development work on the C-5A aircraft had been completed, a series of tests was begun in the three major high-speed wind tunnels in which the majority of transonic tests had been conducted to determine the cause for the differences in aerodynamic data determined from similar configurations. These facilities were the AEDC Propulsion Wind Tunnel (16T), the NASA-Ames Research Laboratory 11-ft Unitary Plan Wind Tunnel, and the Cornell Aeronautical Laboratory 8-ft Transonic Tunnel. The results of the first series of AEDC Propulsion Wind Tunnel Facility (PWT) tests are reported in Ref. 1, and the comparative results from the three participating facilities are presented in Ref. 2.

Although care was taken to provide the best data possible from each facility, potential sources of error were determined to be Mach number measurement and gradient, angle-of-attack measurement, erosion of the boundary-layer trip, and relative tunnel turbulence levels.

In order to more thoroughly investigate and eliminate these potential sources of error and provide what might be considered the best degree of correlation available between transonic wind tunnels, the second series of tests was begun at AEDC in December 1969. This series utilized the identical sting-balance combination used during the first series. Likewise, the same wing-fuselage fillet was maintained for uniformity of the test model. The results of these tests on the wing-fuselage and wing-fuselage-tail configurations at Mach numbers from 0.60 to 0.825 and Reynolds numbers from 2.1×10^6 to 4.2×10^6 are reported herein. The comparative results from the three facilities are presented in Ref. 3.

SECTION II
APPARATUS

2.1 TEST FACILITY

Tunnel 16T is a variable density wind tunnel capable of operating at Mach numbers between 0.20 and 1.60. The tunnel is equipped with a plenum evacuation system, and the test section is formed by fixed, perforated, parallel top and bottom walls and perforated variable angle sidewalls.

For this particular test, very stringent requirements were placed on flow quality and maintenance of tunnel conditions. In order to verify existing tunnel calibration parameters, a supplemental tunnel calibration at Mach numbers from 0.20 to 1.00 was conducted before testing the C-5A model. The results of this tunnel calibration are reported in Ref. 4. An additional investigation was conducted in Tunnel 16T to determine the transition Reynolds number at transonic Mach numbers. Similar investigations using the same equipment were conducted in the Ames 11-ft and the Cornell 8-ft tunnels, thus providing information on the relative turbulence levels of the three participating facilities. The results of the test at AEDC-PWT are given in Ref. 5.

The location of the model and model support system in the test section is shown in Fig. 1, Appendix. A sting support system was utilized to locate the model well forward to avoid any possible strut interference effects. This system placed the aft end of the model approximately 3.4 fuselage lengths forward of the sting support strut.

2.2 TEST ARTICLE

Details of the 0.0226-scale C-5A model are presented in Fig. 2 where the wing-fuselage-tail (WFT) configuration is shown and the individual model components are identified. During the majority of the testing, the tail assembly was removed and replaced with a filler block resulting in the wing-fuselage (WF) configuration. Photographs of configurations WF and WFT installed in the test section are presented in Fig. 3.

Before testing, a detailed inspection of the model was made to determine the angular relationship between the balance centerline and the leveling plate provided for establishing zero angle of attack of the model. The results of the inspection are shown in Fig. 4. Surfaces "A", the bottom of the fuselage beam. "B", a parting line between upper and lower portions of the fuselage beam, and "C", the leveling plate, were found to be parallel to each other. The balance centerline was nose down 0.05 deg relative to these surfaces. Since the participating test facilities had agreed to reduce the aerodynamic coefficients in the balance axes coordinate system, zero angle of attack was defined and established in the tunnel with the balance at 0 deg, model waterlines and the leveling plate at 0.05 deg, and the wing with its 3.5-deg incidence at 3.55 deg.

Previous testing experience with the C-5A had indicated model-balance dynamics which limited the maximum angle of attack at which the model could be tested for certain test conditions. In an attempt to alleviate the dynamics, a viscous damper provided by one of the other test facilities was installed in the model for all tests except for one series of Mach numbers run without the damper to determine its effectiveness. The damper was installed in the model nose cavity.

Transition was fixed on the model by strips of 0.0045-in.-diam glass spheres for all tests except those with free transition. The strips were 0.05 in. wide on the wing and tail surfaces, located with their leading edge 0.8 in. aft streamwise of the leading edge of the model component. the strip on the fuselage was 0.1 in. wide and was located 1 in. aft of the model nose. A photograph of the wing transition strip is shown in Fig. 5a, and a photograph of a representative transition strip from the test of Ref. 1 is shown in Fig. 5b. Comparing these figures, it can be seen that the particle density from the current test was much higher. In order to assess the effects of particle density, the transition material was removed and deliberately reapplied at a density approximately equal to that shown in Fig. 5b. This density was estimated to be one-third to one-half of the previously applied transition strip. Except for the several runs made to determine the effects of particle density and tests of the WFT configuration at $Re = 2.1 \times 10^6$, transition-fixed data were obtained using the high particle density trip.

2.3 INSTRUMENTATION

A six-component, internal, strain-gage balance provided by NASA was used to measure gross forces and moments acting on the model. Pressures in the model cavity were measured at two locations by differential pressure transducers. The model gravimetric angle of attack was measured by a damped, strain-gaged pendulum capable of operating with the model at 0- and 180-deg roll angles. Outputs from the instrumentation were digitized using the PWT instrumentation and reduced on line to coefficient form using the PWT digital computer.

Balance dynamic outputs from all components were continuously recorded on an oscillograph for stress monitoring purposes and for assessment of the effectiveness of the damper.

Seven static pressure orifices were located on the model centerline beginning aft of the cockpit area and extending around to the main wheel well fairing. The orifices were connected to individual transducers, and the measured pressures were converted to coefficients and local Mach numbers. These quantities were for comparison of local flow conditions in all three facilities under the premise that, for identical test conditions, any differences in local conditions could be the result of blockage or possible wall effects.

SECTION III
TEST CONDITIONS AND DATA ACCURACY

3.1 TEST CONDITIONS

The tests were conducted at nominal Mach numbers of 0.600, 0.700, 0.767, 0.785, and 0.825 at Reynolds numbers of 2.1, 2.8, 3.5, and 4.2 million based on the wing mean aerodynamic chord of 0.7 ft. Total temperature was held at 100°F at all Mach numbers. For these test conditions, total pressure ranged from 3835 psfa at M_∞ = 0.600 and Re = 4.2 x 10^6 to 1586 psfa at M_∞ = 0.825 and Re = 2.1 x 10^6. Mach number was closely monitored during testing and was generally held within ±0.001 of the desired value during a polar.

Tunnel conditions were maintained at each Mach number while angle of attack was varied from -4 to 4 deg in 0.5-deg increments; data were recorded at each angle.

3.2 CORRECTIONS

All configurations were tested with the model both upright and inverted to determine model-flow misalignment. Frequent tunnel shutdowns were made to check for instrumentation zero shifts, and corrections were made to the angle-of-attack instrumentation as required. Because of these frequent corrections, no definite trend in possible flow angularity was established; for any selected configuration, indicated model-flow misalignment varied from 0 to a maximum of 0.030 deg. Previous tests have indicated larger model-flow misalignment than that determined during this investigation. Since this test indicated flow angle to be essentially zero, it is very possible that the

previously indicated flow angularity values were the result of procedural errors rather than any undesirable flow quality in the tunnel. Angle of attack was corrected for the indicated model-flow misalignment, and the coefficient data were computed using the corrected angle.

Lift and drag coefficients were computed with the axial force corrected for base pressure effects. The C-5A model geometry resulted in base pressure being greater than free-stream static pressure at all test conditions. No corrections were made to pitching moment for axial-force effects as the moment reference point was located on the balance axis.

Gross forces and moments were corrected for tare effects resulting from model weight acting on the balance. The maximum errors resulting from the weight tare corrections were ±0.2 lb on normal force, ±0.07 lb on axial force, and ±2 in.-lb on pitching moment. The corresponding errors in the coefficients were ±0.00002, ±0.000006, and ±0.0002 on C_N, C_A, and C_m, respectively, at Re = 2.1 x 10^6. At the higher Reynolds numbers, the coefficient errors resulting from these small tare errors were correspondingly reduced.

Reference 2 indicates the possibility of the balance axial-force element being relieved by a thrusting effect of the model resulting from oscillations primarily in the model side-force plane. This effect was extensively investigated by shaking the model in all planes under wind-off conditions both with and without an applied axial force. With the time-averaging instrumentation used at AEDC-PWT for force measurements, no measureable effect was noticed. It was concluded that although a correction of this type had been applied by one of the other participating facilites (Ref. 2), this correction was not applicable for data obtained at AEDC-PWT.

Insufficient time was available between the tunnel calibration indicated in Section 2.1 and the model tests discussed in this report to fully evaluate the calibration results and incorporate any required changes into the tunnel operating procedure. Subsequent evaluation of these results indicated that the actual free-stream Mach numbers were slightly higher than the value computed during this investigation. The amount of the Mach number error is shown in Fig. 6. This ΔM_∞ was added to the computed Mach number to arrive at the true free-stream Mach number. The resulting change in dynamic pressure was less than 1 psf which in turn reduced C_A (or C_D) less than 0.00004. The calibration results also indicated a slight static pressure gradient in the portion of the tunnel occupied by the C-5A model. This resulted in the buoyancy corrections shown in Fig. 7 which were applied to the data. Since the ΔM_∞ correction resulted in a ΔC_D of opposite sign to that of the buoyancy correction, the net ΔC_D corrections were less than 0.0001.

3.3 ACCURACY OF MEASUREMENTS

The extreme care with which the test was conducted resulted in coefficient and tunnel condition uncertainties which were quite low. The uncertainties presented are for M_∞ = 0.767 and a Reynolds number of 2.1 x 10^6. At test conditions of higher dynamic pressure, the coefficient uncertainties would be reduced. The accuracies were as follows:

M_∞	±0.001
α	±0.02 deg
C_N	±0.002
C_L	±0.002
C_A	±0.0003
C_D	±0.0004
C_{D_b}	±0.0001
C_m	±0.001

SECTION IV
RESULTS AND DISCUSSION

4.1 TRANSITION STRIP PARTICLE DENSITY EFFECTS

The effects of transition strip particle density are presented in Fig. 8. Free transition data are also shown for comparative purposes. These data show that for $C_L \leq 0.5$, variation in transition strip density was of small consequence, but for higher values of C_L, the data obtained with the lower grit density approached the free transition data. At lower Mach numbers, this effect would probably not be as severe but would be accentuated at $M_\infty > 0.767$ where wing shocks would be stronger. The effects on C_A were less pronounced than on C_L or C_m, but decreasing the grit density reduced C_A by 0.0014 at $C_N = 0.7$. This combined with the lower α required for a constant C_L would lower C_D by 0.0087 at $C_L = 0.7$. Although a C_L of 0.7 is well above the cruise value for the C-5A at $M_\infty = 0.767$, it could fall well within the flight envelope of other types of aircraft.

The impact of this brief investigation lies in the necessity of close duplication in grit application whether it be for correlation between different wind tunnels or ordinary reapplication of grit during a wind tunnel test. If reasonable duplication is not maintained, erroneous conclusions could be derived from the test results.

4.2 EFFECTS OF REYNOLDS NUMBER VARIATION FOR THE WF CONFIGURATION; FREE AND FIXED TRANSITION

The WF configuration was tested with transition fixed at four Reynolds numbers between 2.1×10^6 and 4.2×10^6 and with transition free at Reynolds numbers 2.1×10^6 and 2.8×10^6. These data are presented in Figs. 9 through 12.

Figure 9a shows that with transition fixed, Reynolds number variation had very little effect on C_L, particularly at $C_L \leq 0.55$. At higher angles of attack corresponding to $C_L > 0.55$, there was a slight increase in C_L with increased Reynolds number. The free transition data, although determined at only two Reynolds numbers, showed greater effects of Reynolds number variation; the higher Reynolds number produced significantly higher values of C_L at $\alpha > 2$ deg. Comparison of the free and fixed transition data shows that at $M_\infty = 0.600$ and 0.700, C_L became coincident at $\alpha = 2$ deg and then diverged as α was increased; the free transition data indicated less tendency toward stall.

The pitching-moment coefficients (Fig. 9a) with transition fixed became more negative in an essentially linearly decreasing manner as Re was increased at all Mach numbers and

angles of attack except those near the extremes of the angle-of-attack range. The free transition data showed no effect of Reynolds number at $M_\infty \leq 0.70$ but showed large and differing effects at $M_\infty > 0.70$; the low Reynolds number data indicated more negative C_m at lift coefficients approaching 0.25 to 0.30 and more positive C_m at higher values of C_L. Comparison of the two families of curves shows that at $M_\infty \leq 0.700$, C_m, like C_L, became coincident at α = 2 deg, but for $M_\infty > 0.700$, the free transition C_m remained much more negative and showed less tendency toward stall.

The axial-force coefficients presented in Fig. 9b show that with transition fixed, C_A generally decreased with increasing Reynolds number at all Mach numbers and normal-force coefficients. The free transition data generally showed a similar trend except for C_N greater than approximately 0.5 where Reynolds number had little effect.

The drag polars presented in Fig. 9c show the expected trend of decreasing C_D with increasing Reynolds number for all test conditions. The very large drag reduction shown at the higher values of C_L for the configuration with free transition was a result not only of the reduction in C_A with free transition but of the significantly lower α required to attain a given C_L. At the previously mentioned conditions where C_L values for fixed and free transition were equal, the reduced drag resulted only from the reduced C_A. Base drag coefficient was invariant with Reynolds number and showed essentially no effect of transition method.

A summary of the lift and drag characteristics of the WF configuration is presented in Figs. 10, 11, and 12. The lift data (Fig. 10) confirmed that for fixed transition, Reynolds number effects were very small, exhibiting only a slight increase in C_{L_o} and C_{L_α} with increased Reynolds number. For free transition, increasing Reynolds number resulted in a more positive α_{L_o}; C_{L_o} and C_{L_α} were essentially unaffected.

The variation of C_D with Mach number with transition fixed at all values of C_L and transition free at $C_L \leq 0.2$ exhibited the phenomenon of steadily increasing drag with Mach number for all values of Reynolds number. This characteristic, which may be peculiar to the C-5A, had been previously noted in testing and was given the term "creep drag" by the Lockheed-Georgia Company. Although determination of a drag divergence Mach number with transition fixed is made more difficult by the "creep drag," a comparison of the fixed and free transition data shows that free transition testing would produce a drag divergence Mach number higher than that determined with transition fixed.

The variation of C_D with Reynolds number presented in Fig. 12 represents a cross plot from Fig. 9 and shows, within the accuracy of the data, a linear decrease in C_D with increasing Reynolds number.

4.3 EFFECTS OF REYNOLDS NUMBER VARIATION FOR THE WFT CONFIGURATION, FIXED TRANSITION

The effects of Reynolds number variation on the aerodynamic characteristics of the wing-fuselage-tail configuration are presented in Figs. 13 through 15. This configuration

was tested only with transition fixed and, as mentioned in Section 2.2, the data at Re = 2.1 x 10^6 were obtained with the light transition particle density.

The lift coefficient data showed only small effects of Reynolds number variation at $C_L \leq 0.4$. At higher angles of attack, increasing Reynolds number produced slightly higher C_L. The effects of the less dense boundary-layer trips are evident at the higher angles of attack where the Re = 2.1 x 10^6 data exhibited trends similar to that discussed in Section 4.1.

The pitching-moment coefficients (Fig. 13b) showed no effect of either Reynolds number variation or transition particle density at $M_\infty = 0.600$. As Mach number was increased, the pitching moment determined with the less dense grit application and at the lowest Reynolds number generally exhibited a less stable trend. The cause of this occurrence is difficult to determine as the pitching-moment data for the configuration with tail on exhibited more scatter than the configuration with tail off.

The axial-force coefficients presented in Fig. 13c show that axial force was reduced as Reynolds number was increased at all test conditions except for $C_N > 0.45$ at $M_\infty = 0.825$ where the Re = 2.1 x 10^6 and 2.8 x 10^6 data were essentially identical. The drag coefficients (Fig. 13d) show a similar reduction with increasing Reynolds number except for $C_L > 0.50$ and $M_\infty > 0.767$. At these higher lift coefficients and Mach numbers, the normal-force contribution to drag resulting from the higher α required for a constant C_N (or C_L) was greater than the drag reduction caused by increasing Reynolds number. At the angles of attack and normal-force coefficients being considered, a disparity of 0.1 deg in α can contribute 0.0011 in C_D. If this drag contribution is not considered, the erroneous conclusion could be drawn that C_D increased as Reynolds number was increased.

The lift characteristics summarized in Fig. 14 for configuration WFT indicate greater Reynolds number effects than did those for configuration WF. The angle of attack for zero lift (α_{L_0}) became more negative, and the lift coefficient at $\alpha = 0$ (C_{L_0}) became more positive as Reynolds number was increased. The lift coefficient slope (C_{L_α}) remained essentially invariant with Reynolds number, thus indicating a slight increase in lift at constant angle of attack with increased Reynolds number.

The variation of C_D with Mach number (Fig. 15) exhibited greater effect of "creep drag" than did the WF configuration data presented in Fig. 11.

The variation of C_D with Reynolds number presented in Fig. 16 showed a very linear decrease in C_D with increasing Reynolds number at all test conditions.

REFERENCES

1. Black, J. A. and Shadow, T. O. "Effects of Reynolds Number Variation on the Stability and Axial-Force Characteristics of a 0.0226-Scale Model of the C-5A Aircraft at Mach Numbers 0.700, 0.767, and 0.785." AEDC-TR-67-265 (AD823977), December 1967.

2. Treon, Stuart L., Steinle, Frank W., Hofstetter, William R. and Hagerman, John R. "Data Correlation from Investigations of a High-Subsonic Speed Transport Aircraft Model in Three Major Transonic Wind Tunnels." AIAA Preprint No. 69-794, July 1969.

3. Treon, Stuart L., Steinle, Frank W., Hagerman, John R., Black, John A., and Buffington, Robert J. "Further Correlation of Data from Investigations of a High-Subsonic Speed Transport Aircraft Model in Three Major Transonic Wind Tunnels." AIAA Paper No. 71-291, March 1971.

4. Jackson, F. M. "Supplemental Calibration Results for the AEDC Propulsion Wind Tunnel (16T)." AEDC-TR-70-163 (AD872475), August 1970.

5. Credle, O. P. and Carelton, W. E. "Determination of Transition Reynolds Number in the Transonic Mach Number Range." AEDC-TR-70-218 (AD875995), October 1970.

APPENDIX
ILLUSTRATIONS

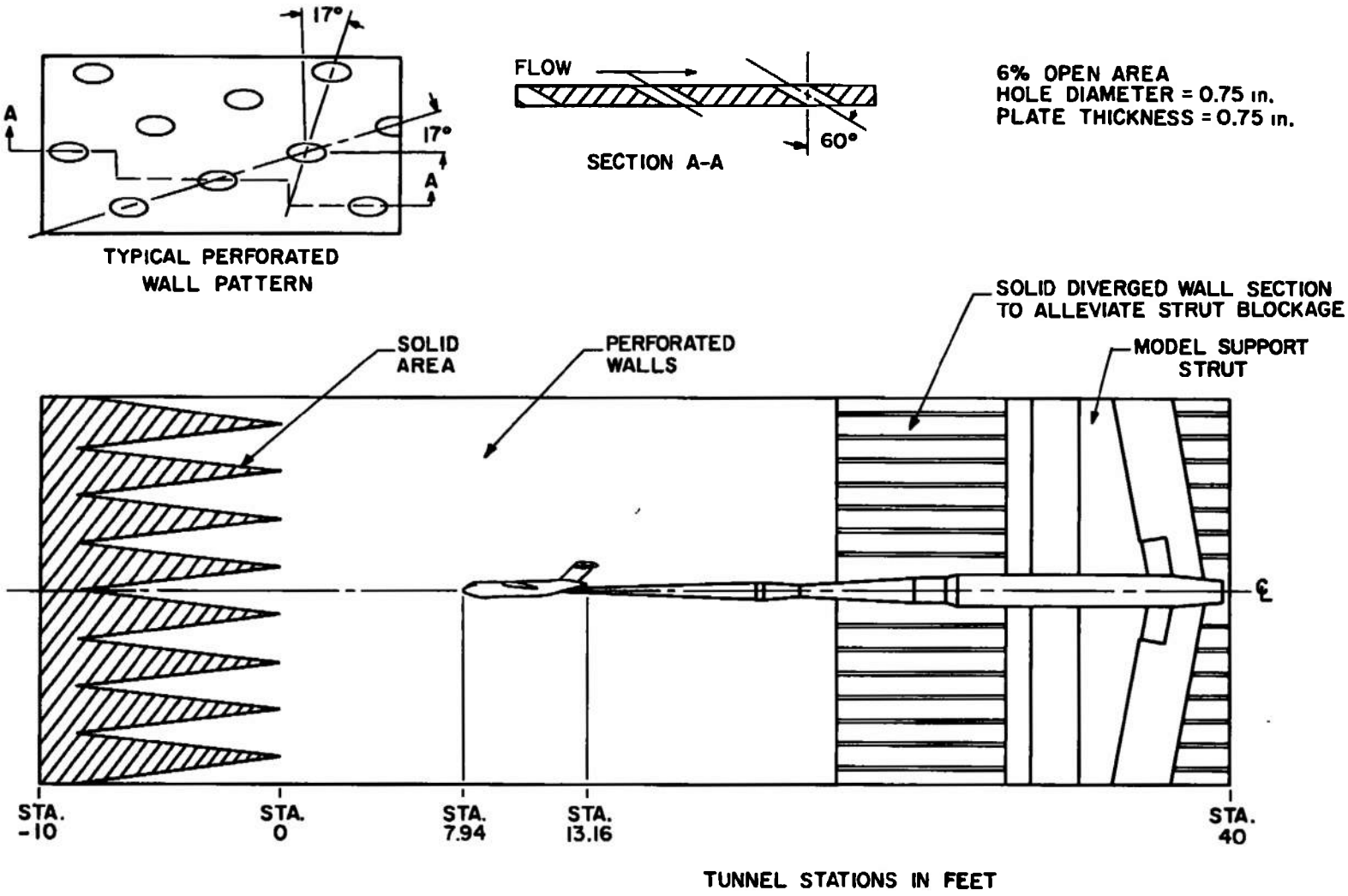

Fig. 1 Sketch of Model Installation

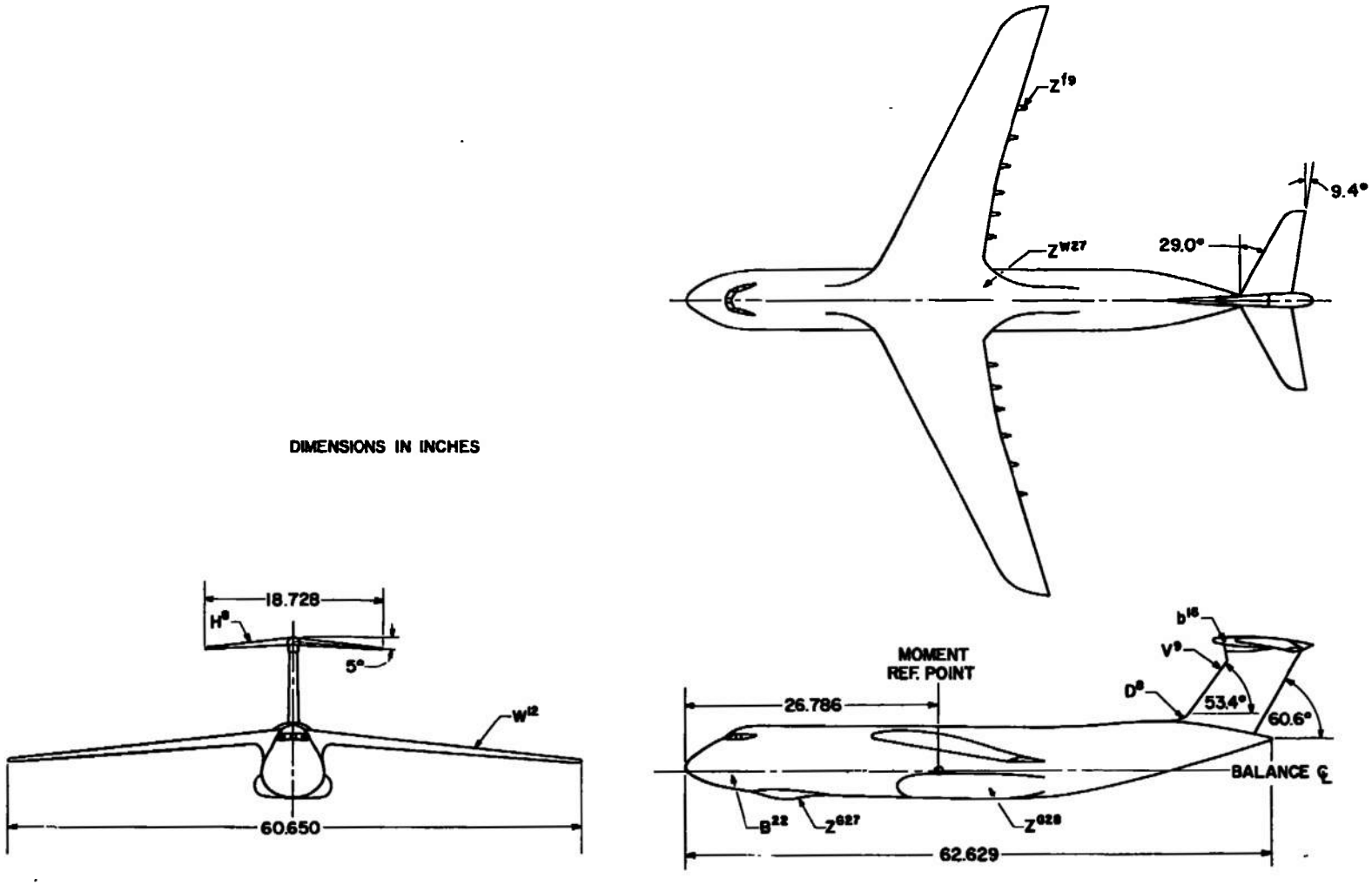

Fig. 2 Model Details and Dimensions

a. Wing-Fuselage Configuration

Fig. 3 Photographs of Models in the Test Section

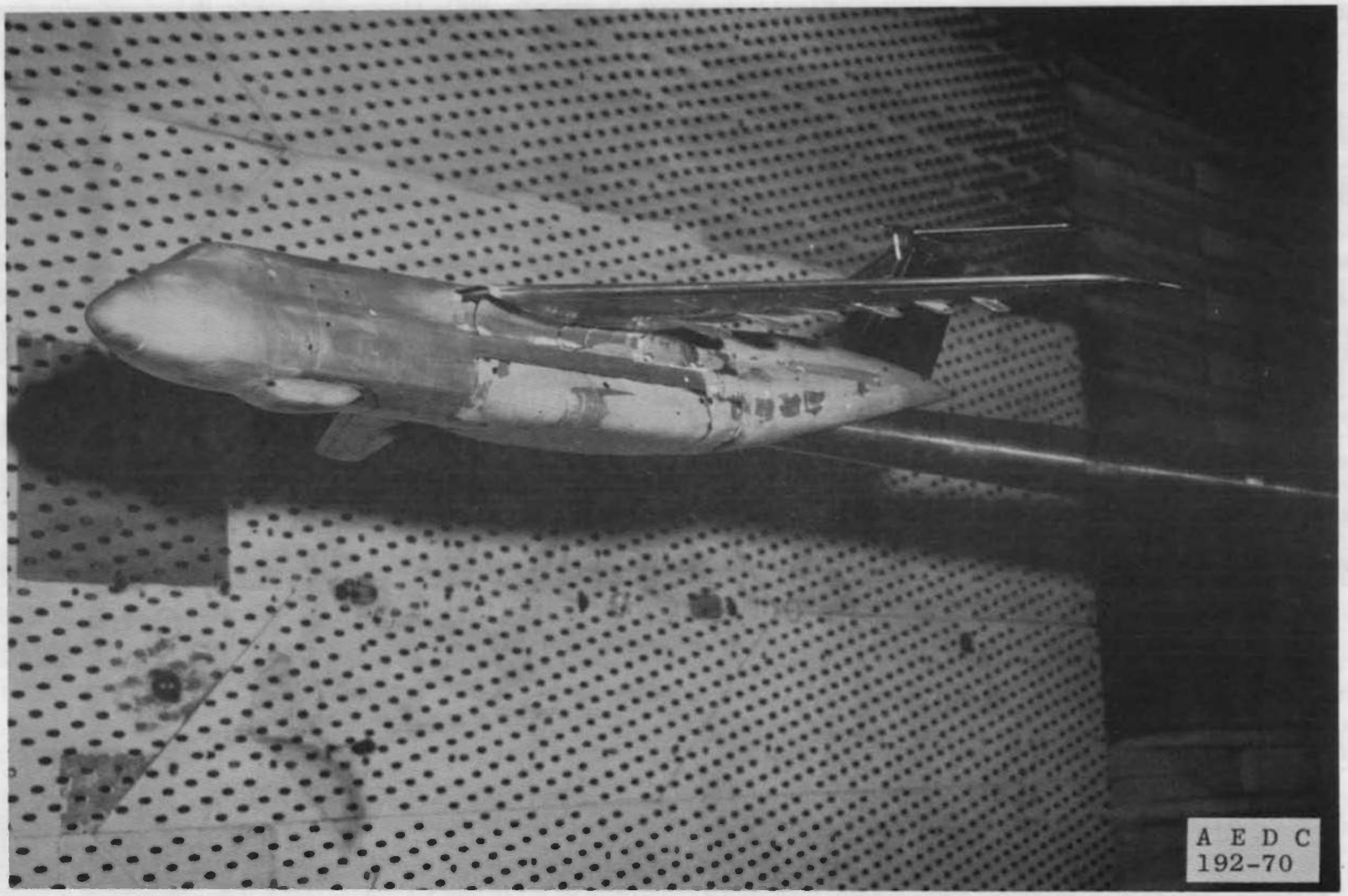

b. Wing-Fuselage-Tail Configuration
Fig. 3 Continued

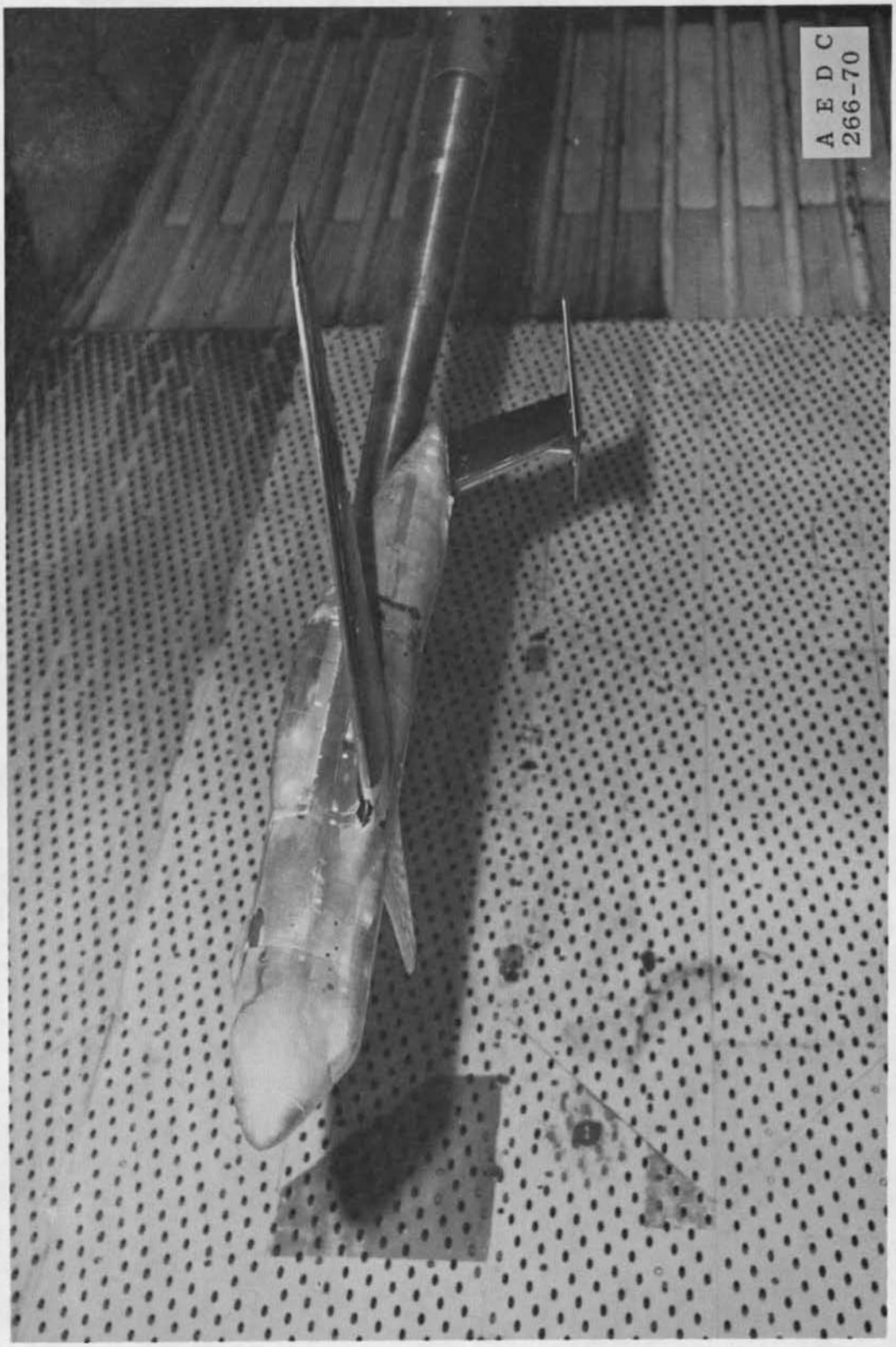

c. Wing-Fuselage-Tail Configuration Inverted
Fig. 3 Concluded

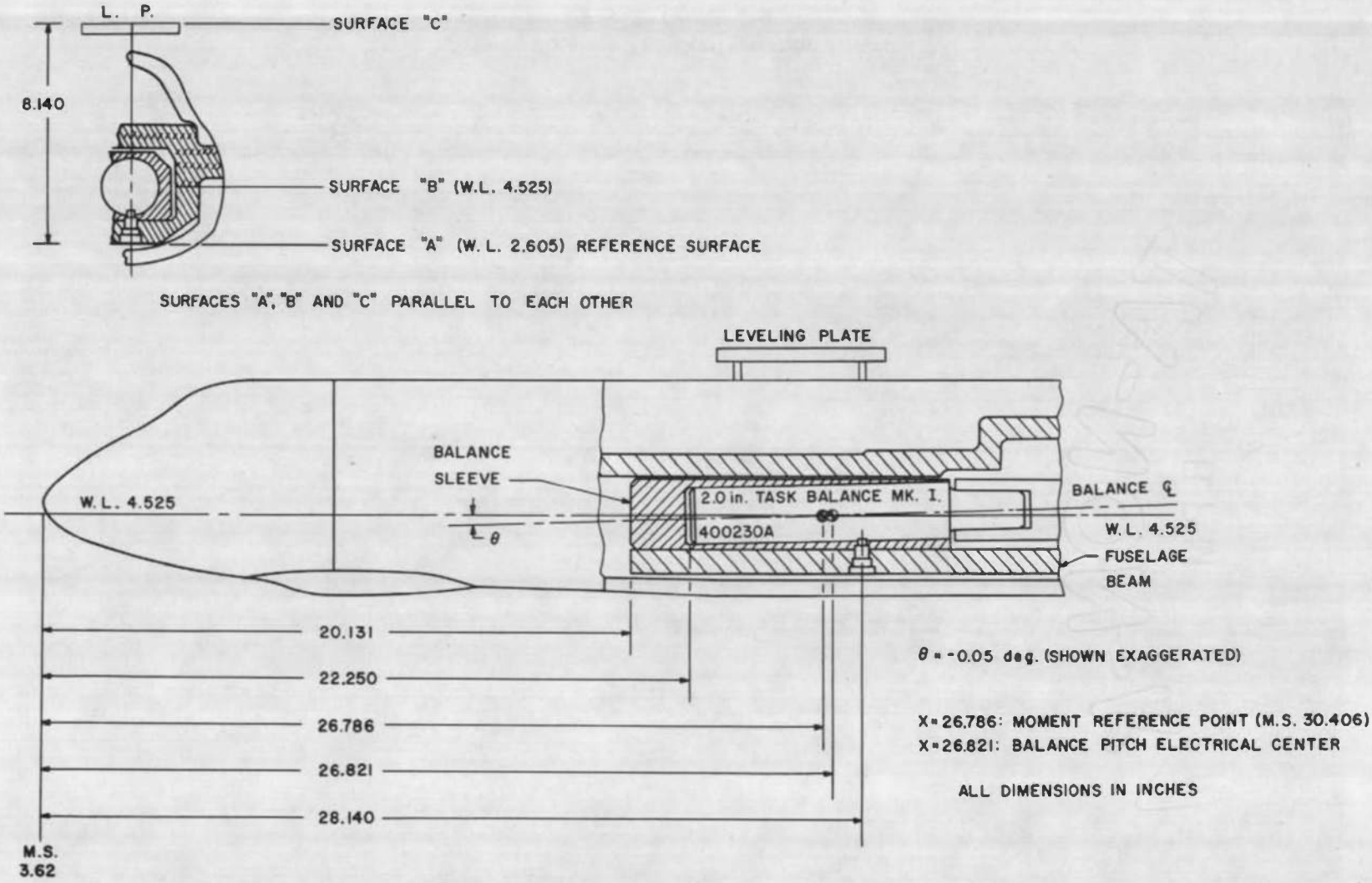

Fig. 4 Sketch of Model-Balance Relationship

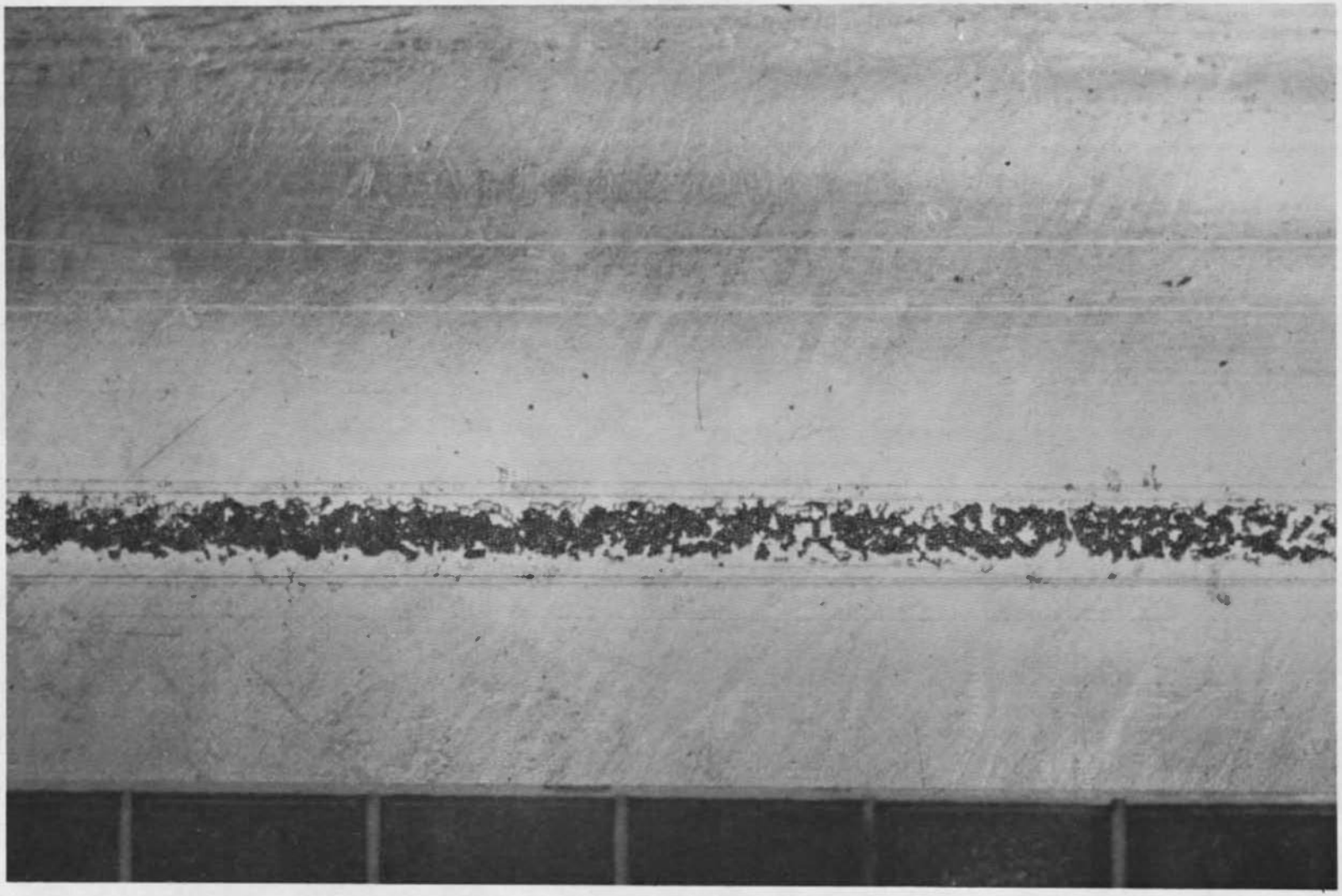

a. Current Test

Fig. 5 Photographs of Transition Strip Particle Density

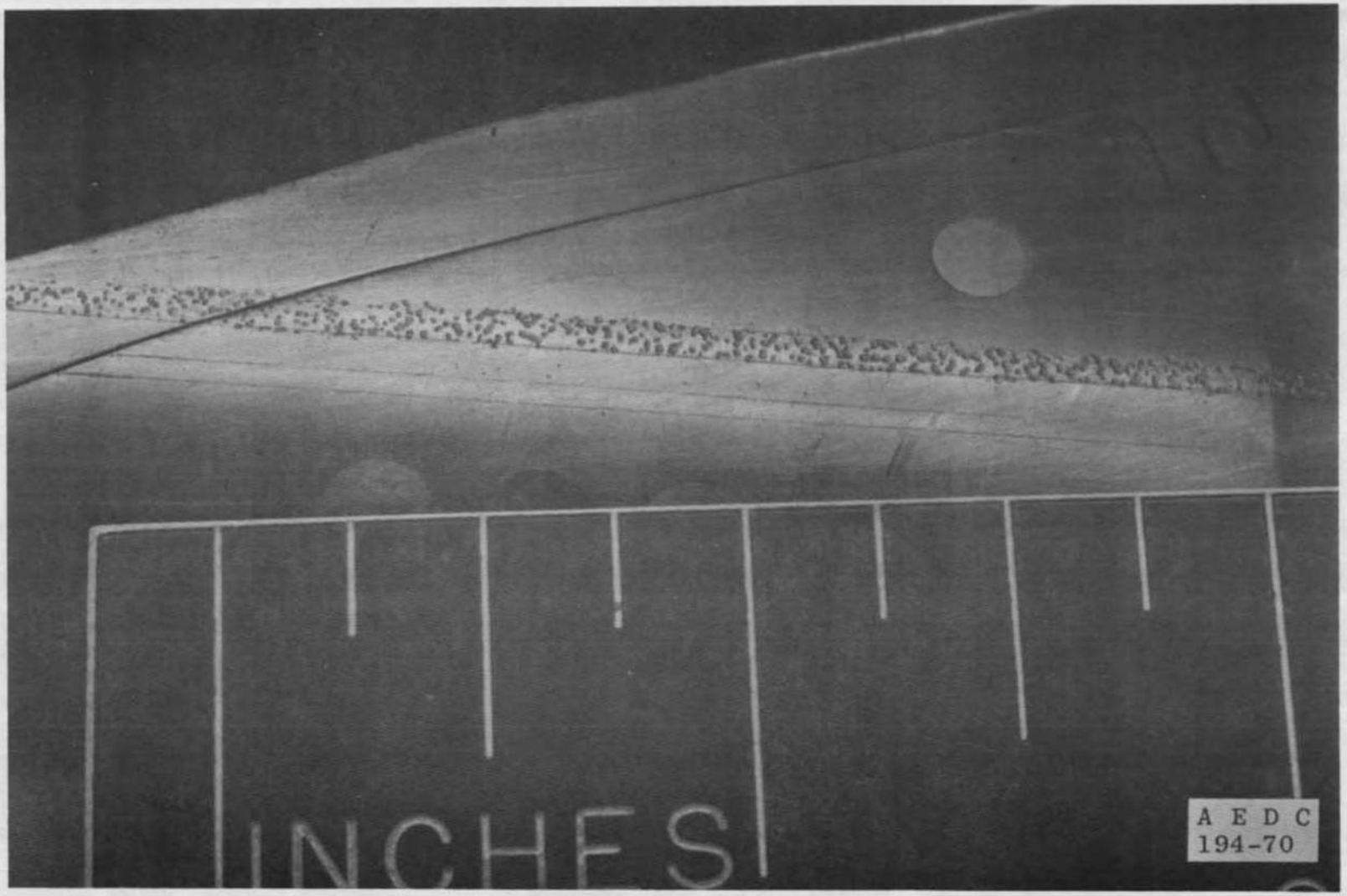

b. Reference 1 Test
Fig. 5 Concluded

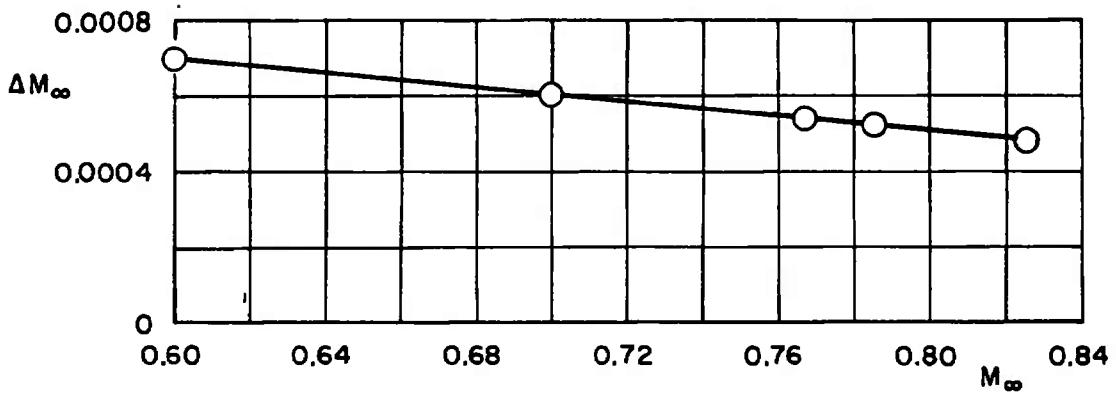

Fig. 6 Mach Number Correction

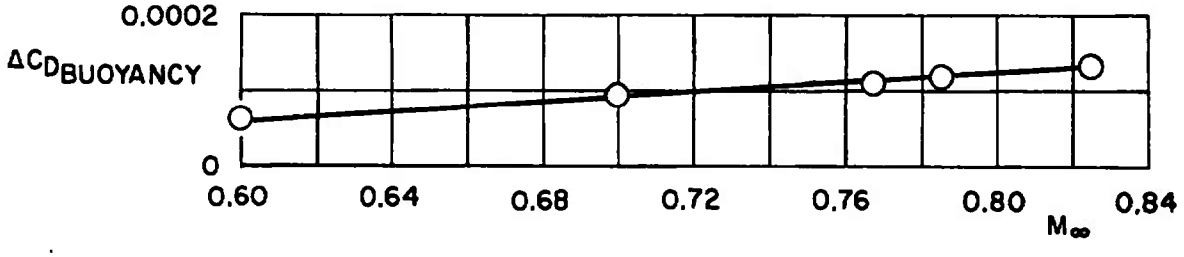

Fig. 7 Drag Correction for Buoyancy Effects

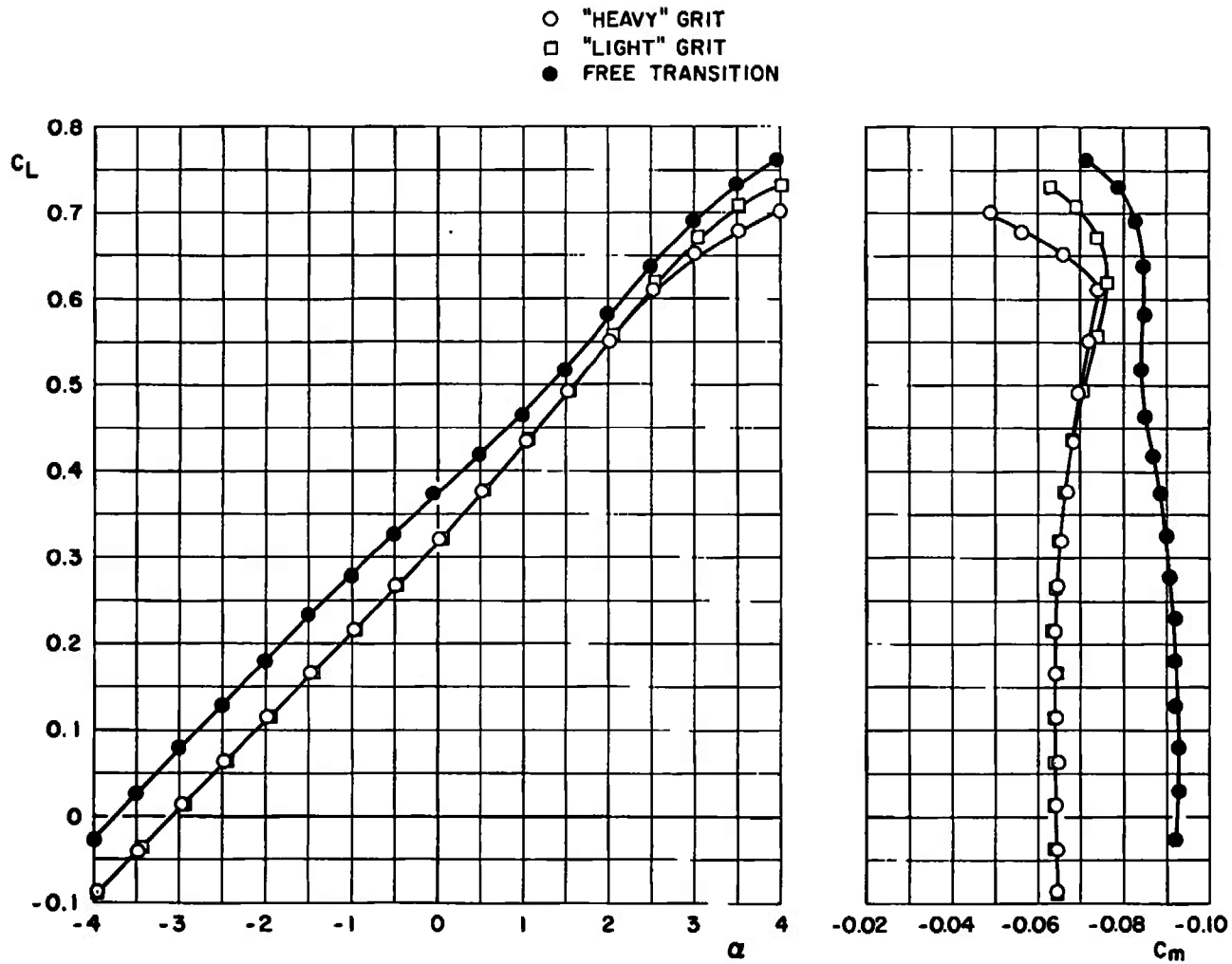

a. C_L and C_m

Fig. 8 Effects of Transition Strip Particle Density on the Aerodynamic Coefficients of the Wing-Fuselage Configuration at M_∞ = 0.767, Re = 2.1 x 10^6

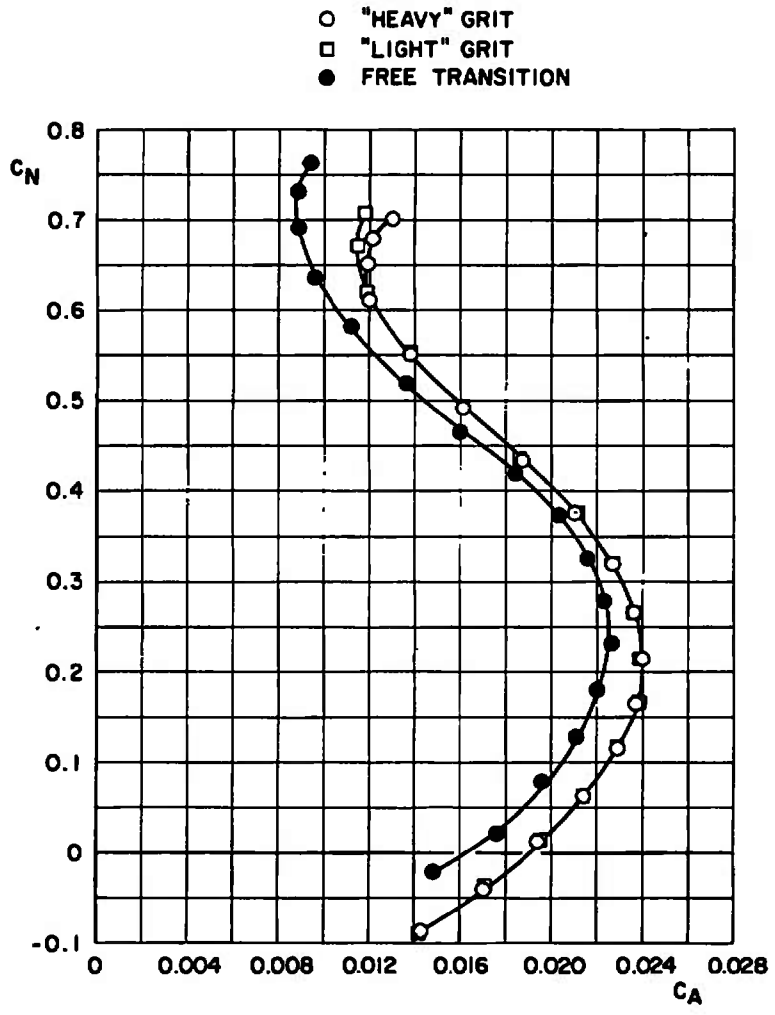

b. C_A

Fig. 8 Concluded

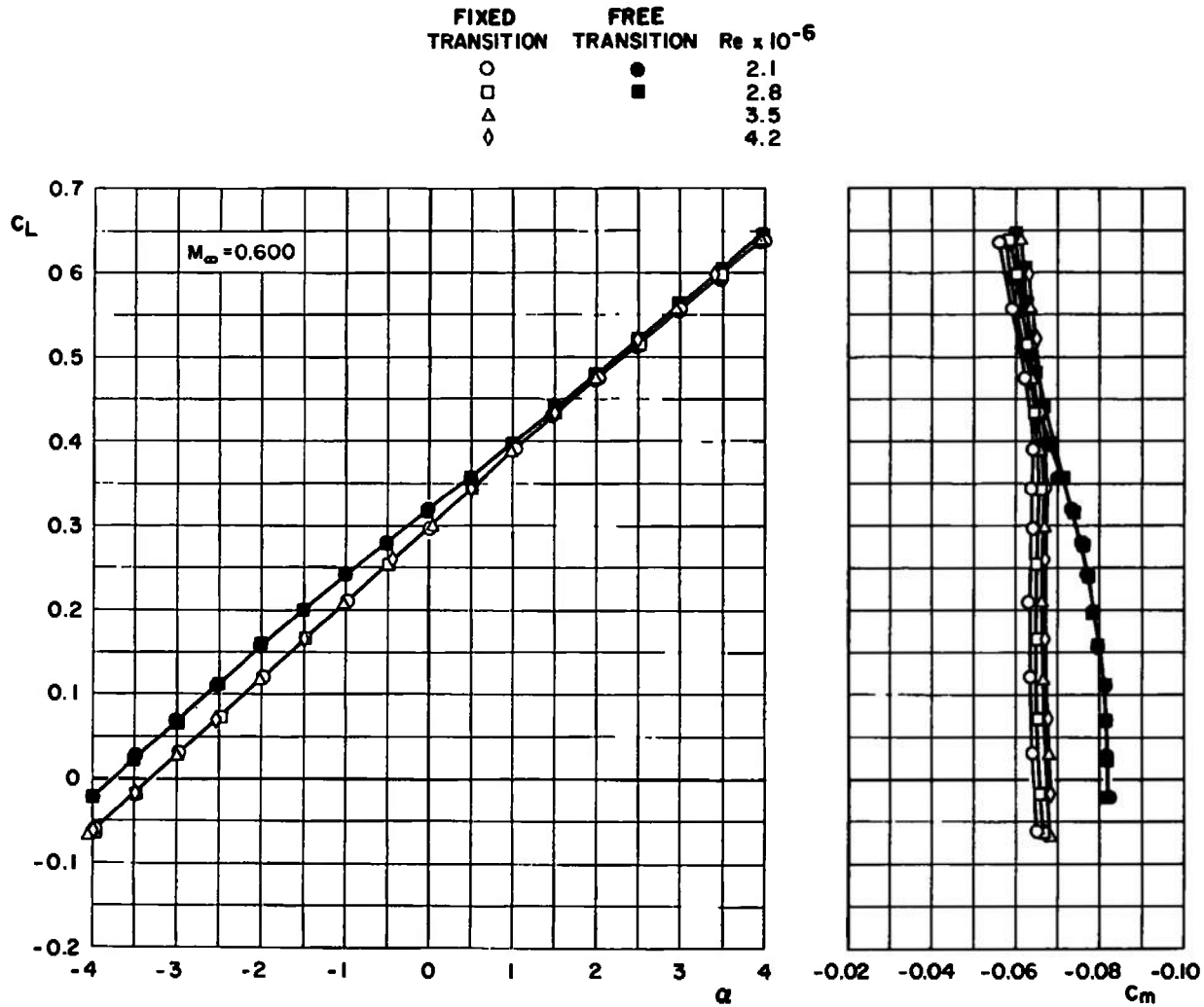

a. C_L and C_m

Fig. 9 Effects of Reynolds Number Variation on the Aerodynamic Coefficients of the Wing-Fuselage Configuration at Mach Numbers from 0.600 to 0.825

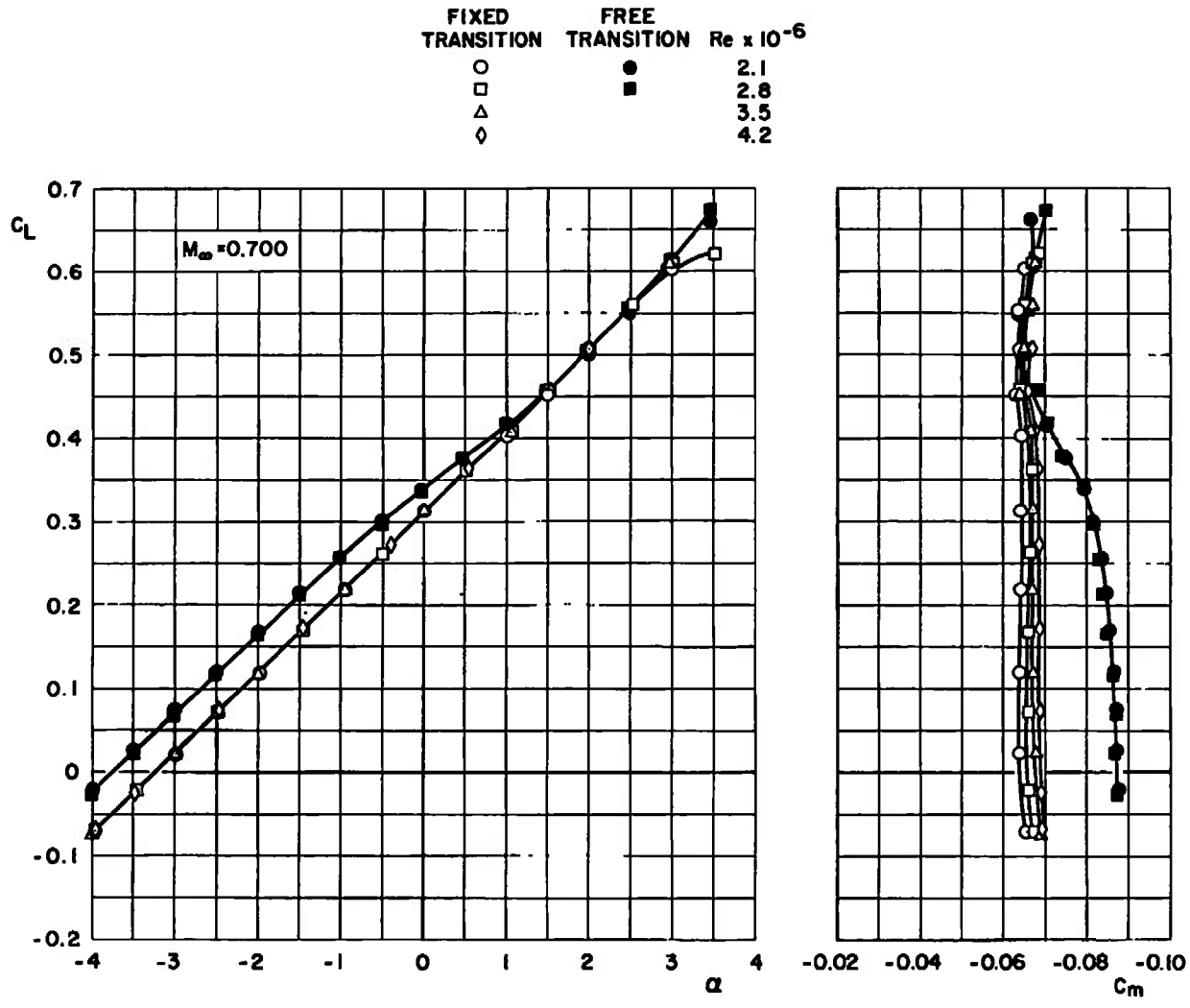

a. Continued

Fig. 9 Continued

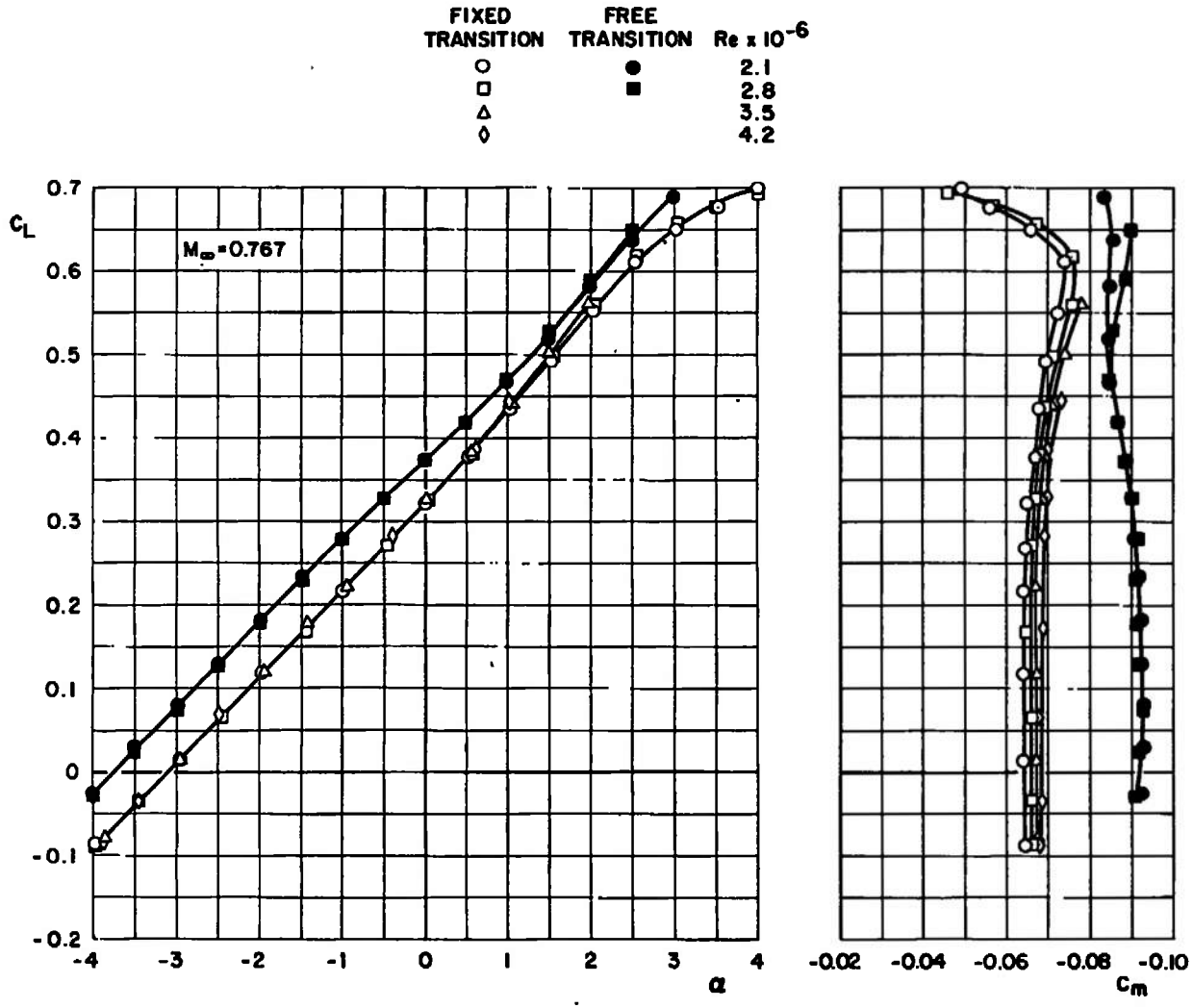

a. Continued
Fig. 9 Continued

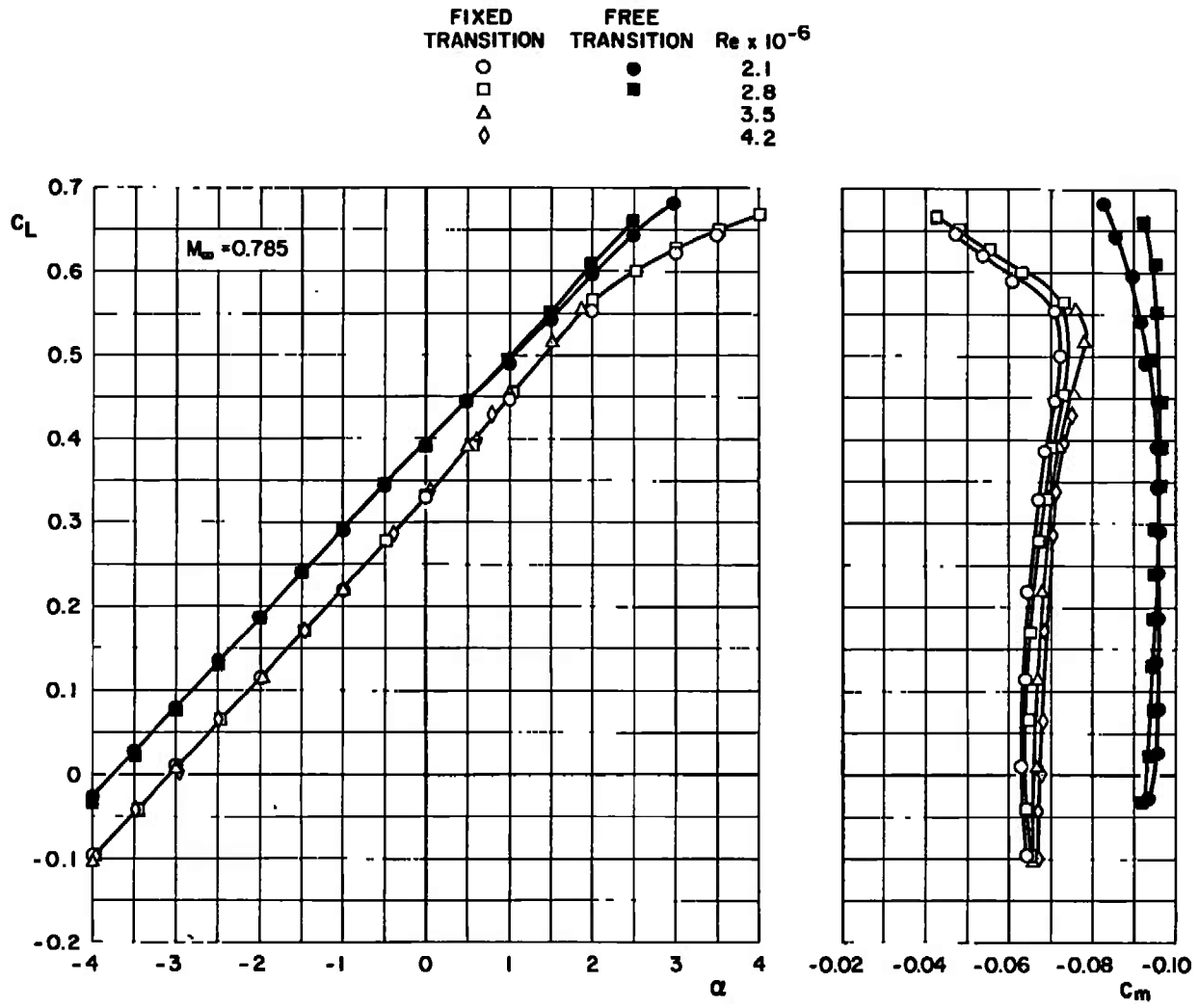

a. Continued

Fig. 9 Continued

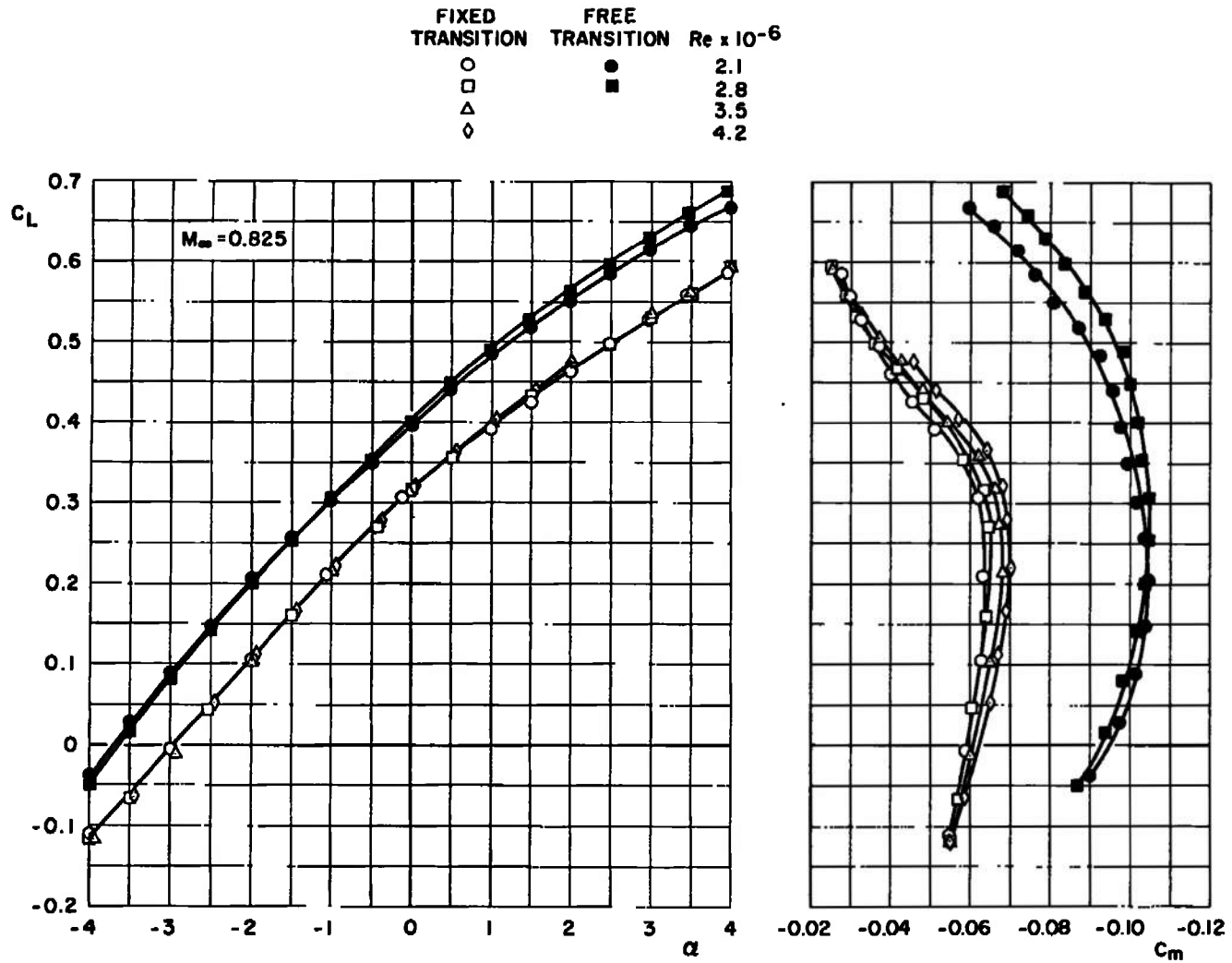

a. Concluded

Fig. 9 Continued

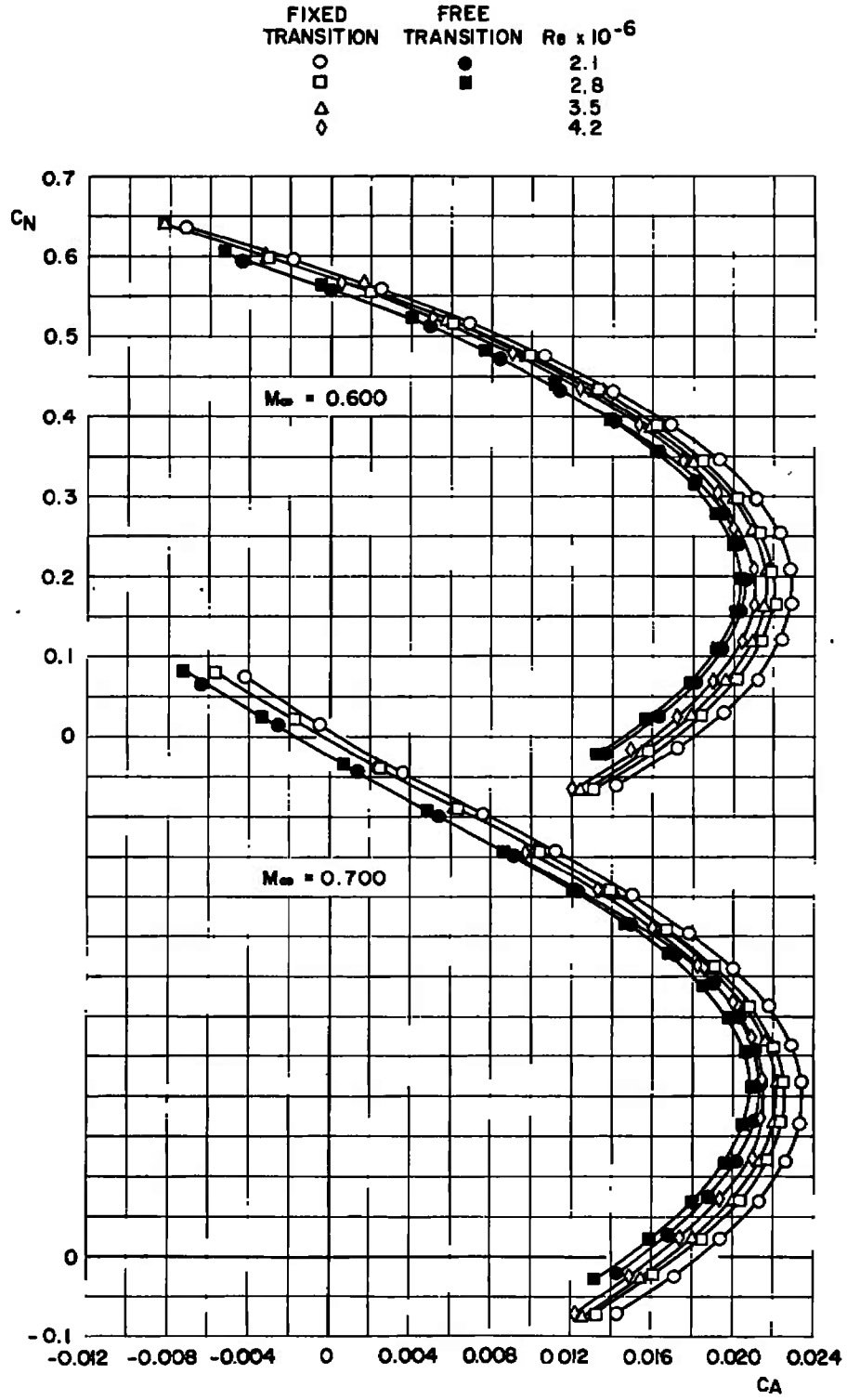

b. C_A

Fig. 9 Continued

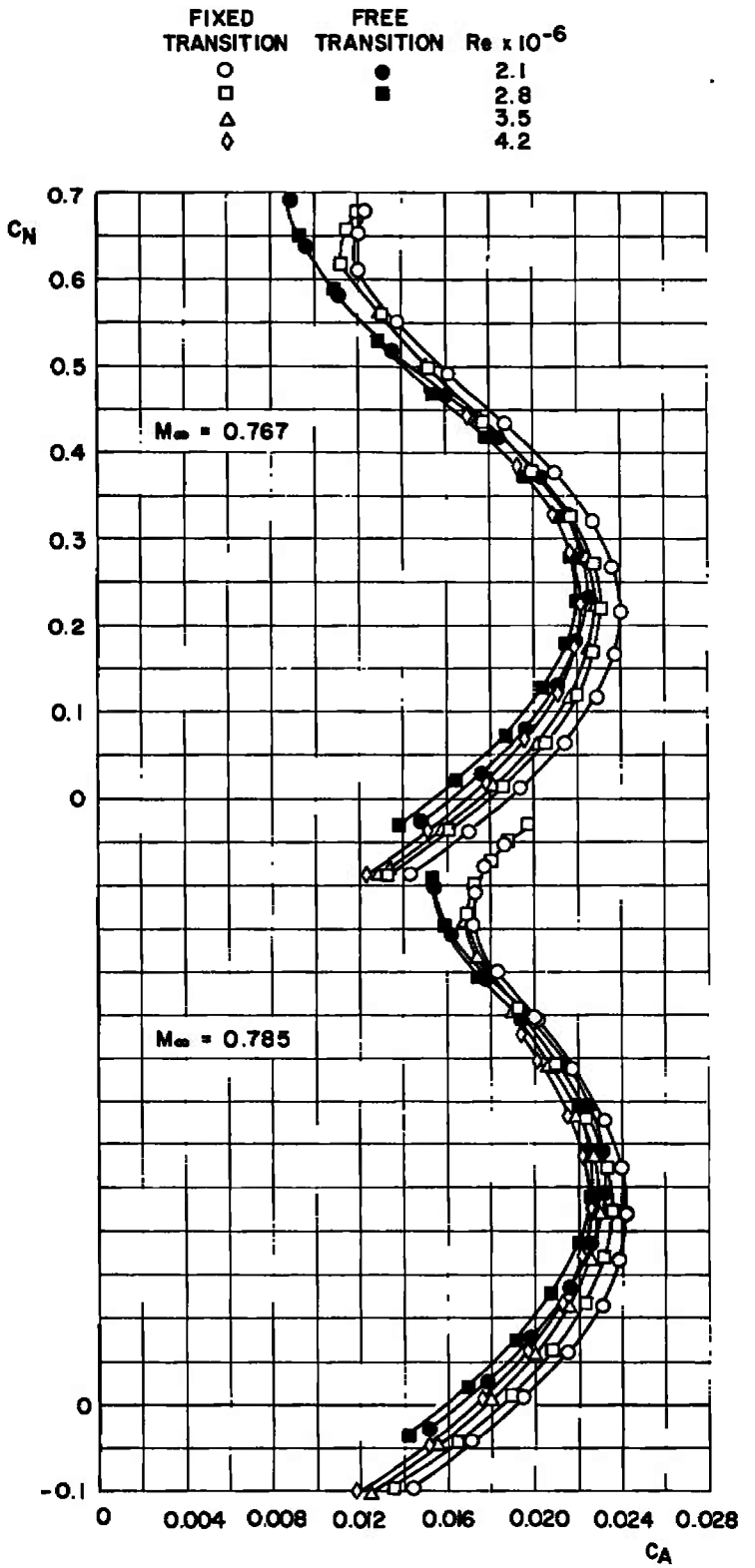

b. Continued
Fig. 9 Continued

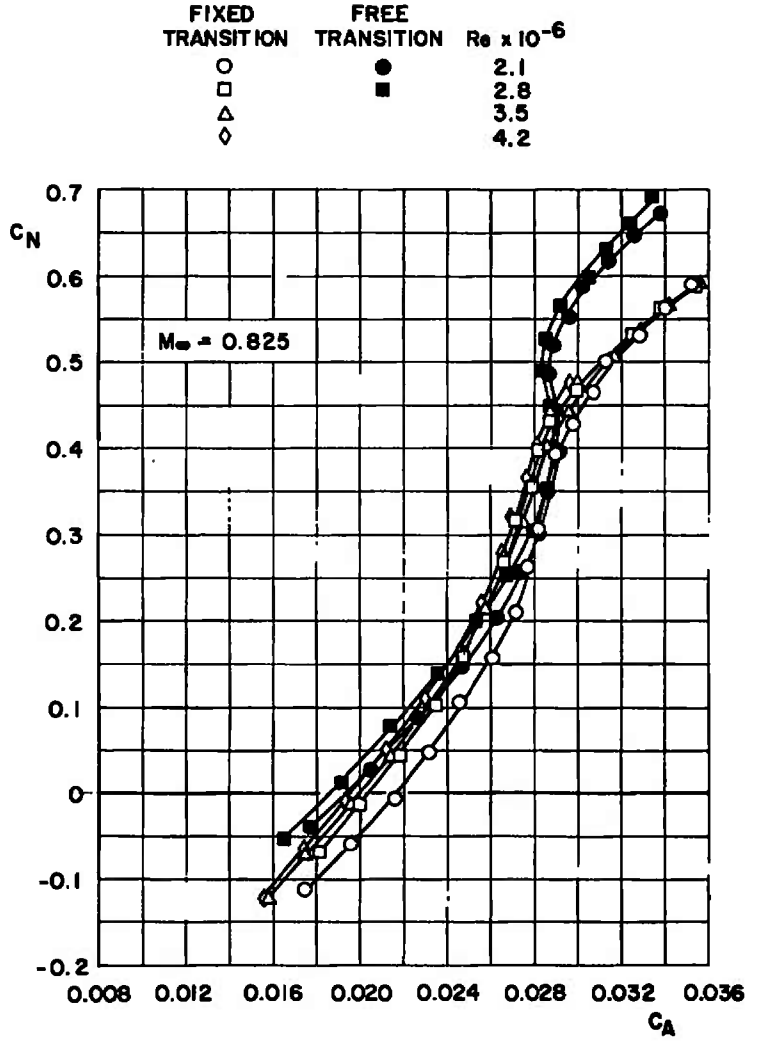

b. Concluded
Fig. 9 Continued

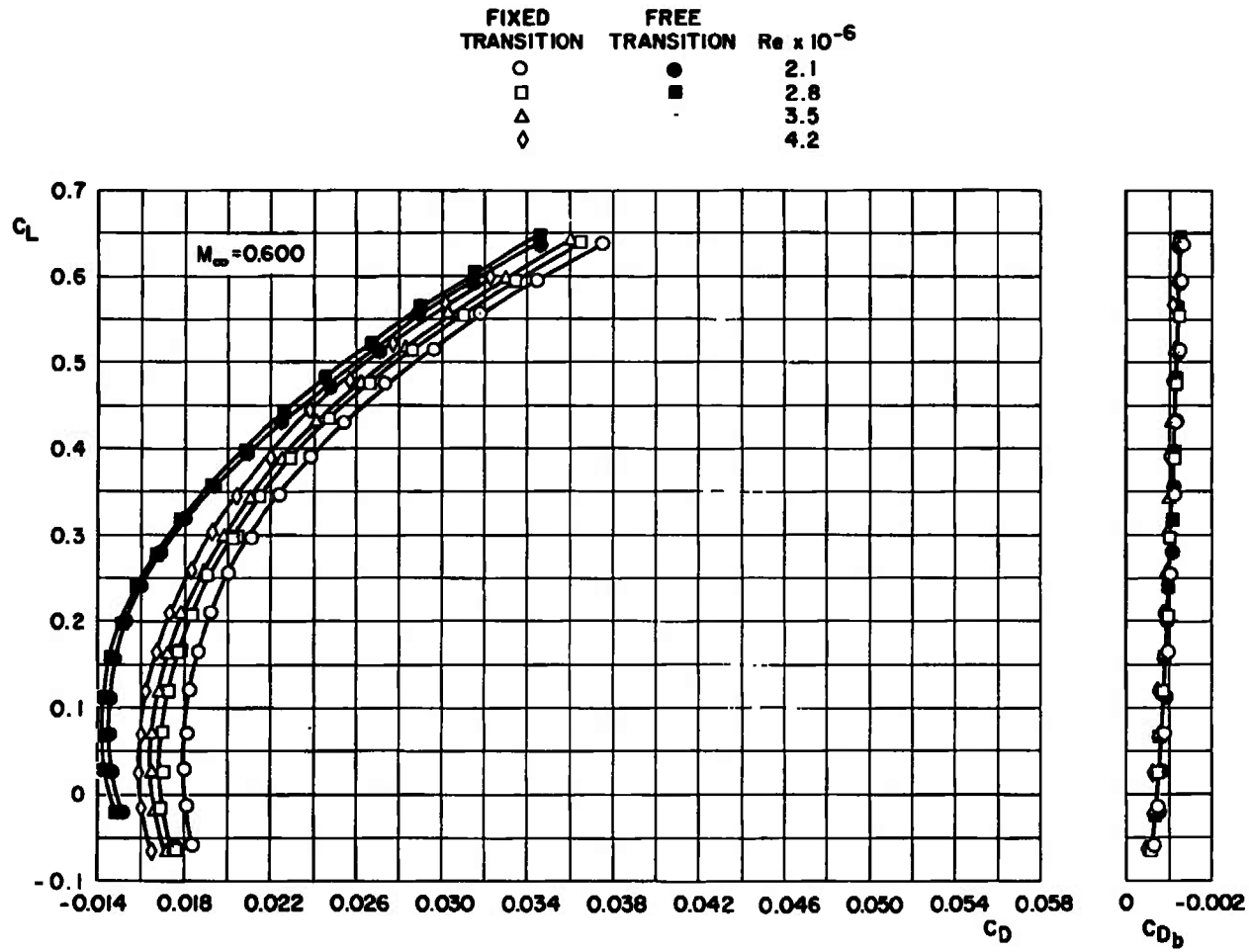

c. C_D and C_{D_b}
Fig. 9 Continued

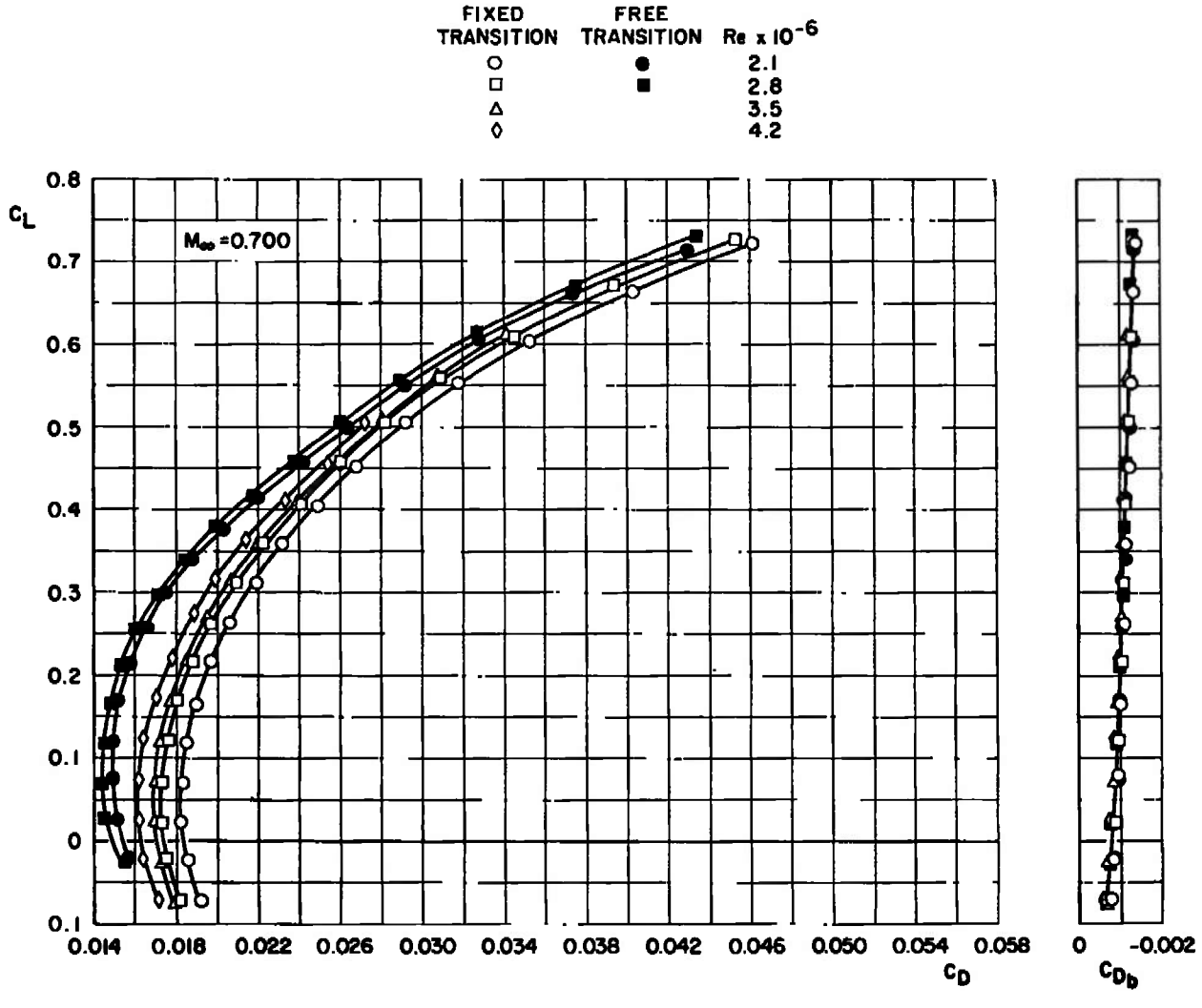

c. Continued

Fig. 9 Continued

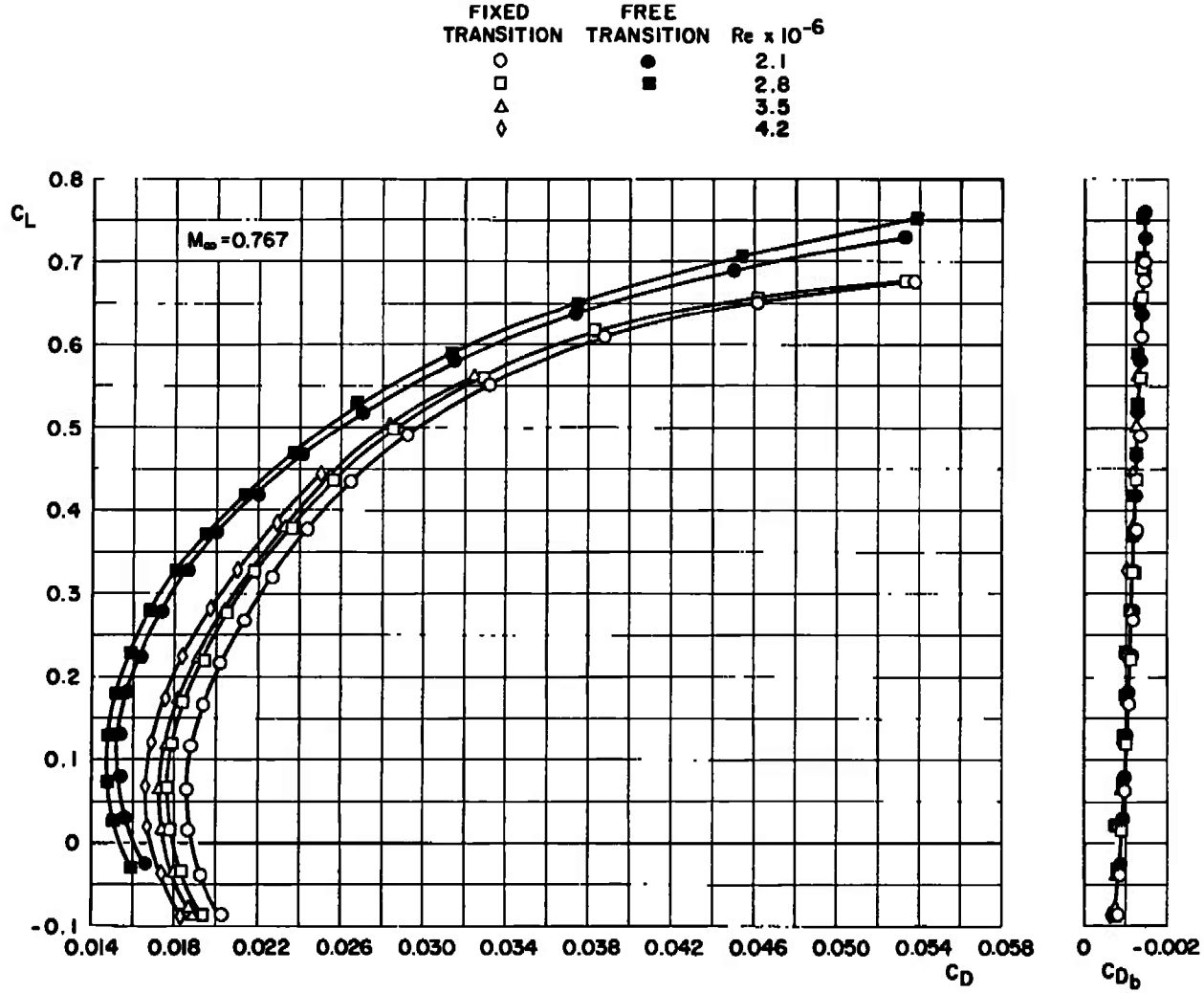

c. Continued

Fig. 9 Continued

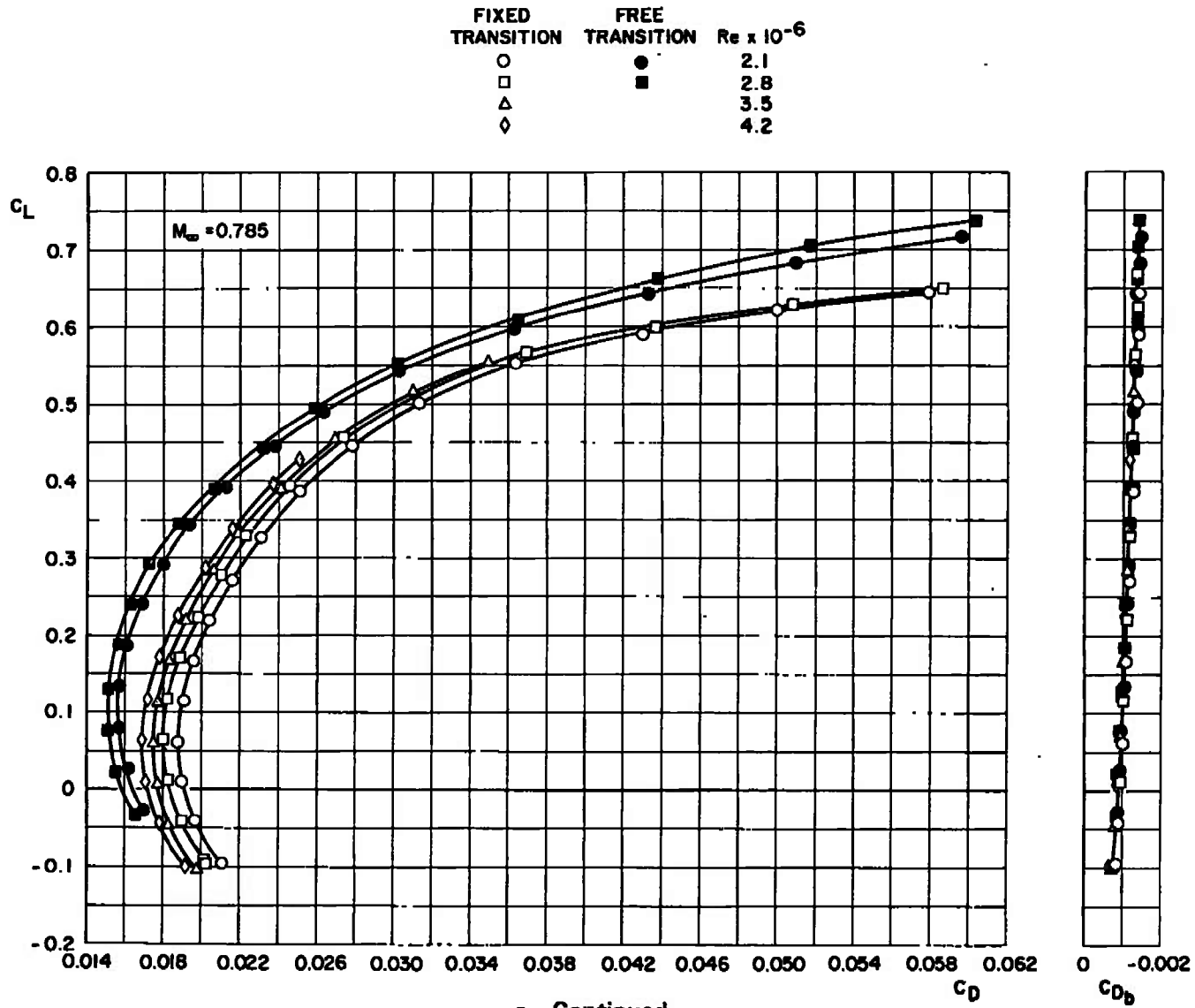

c. Continued

Fig. 9 Continued

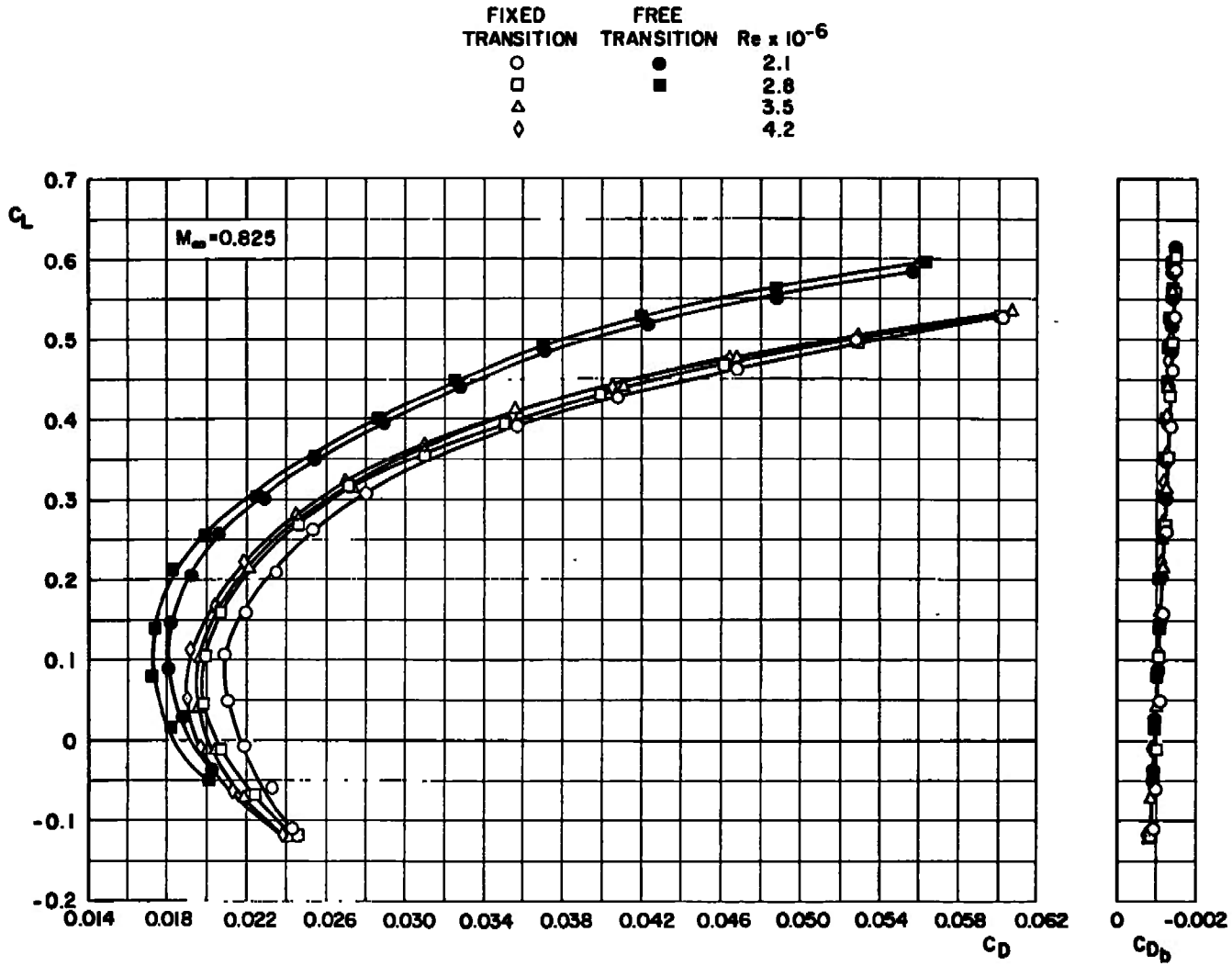

c. Concluded

Fig. 9 Concluded

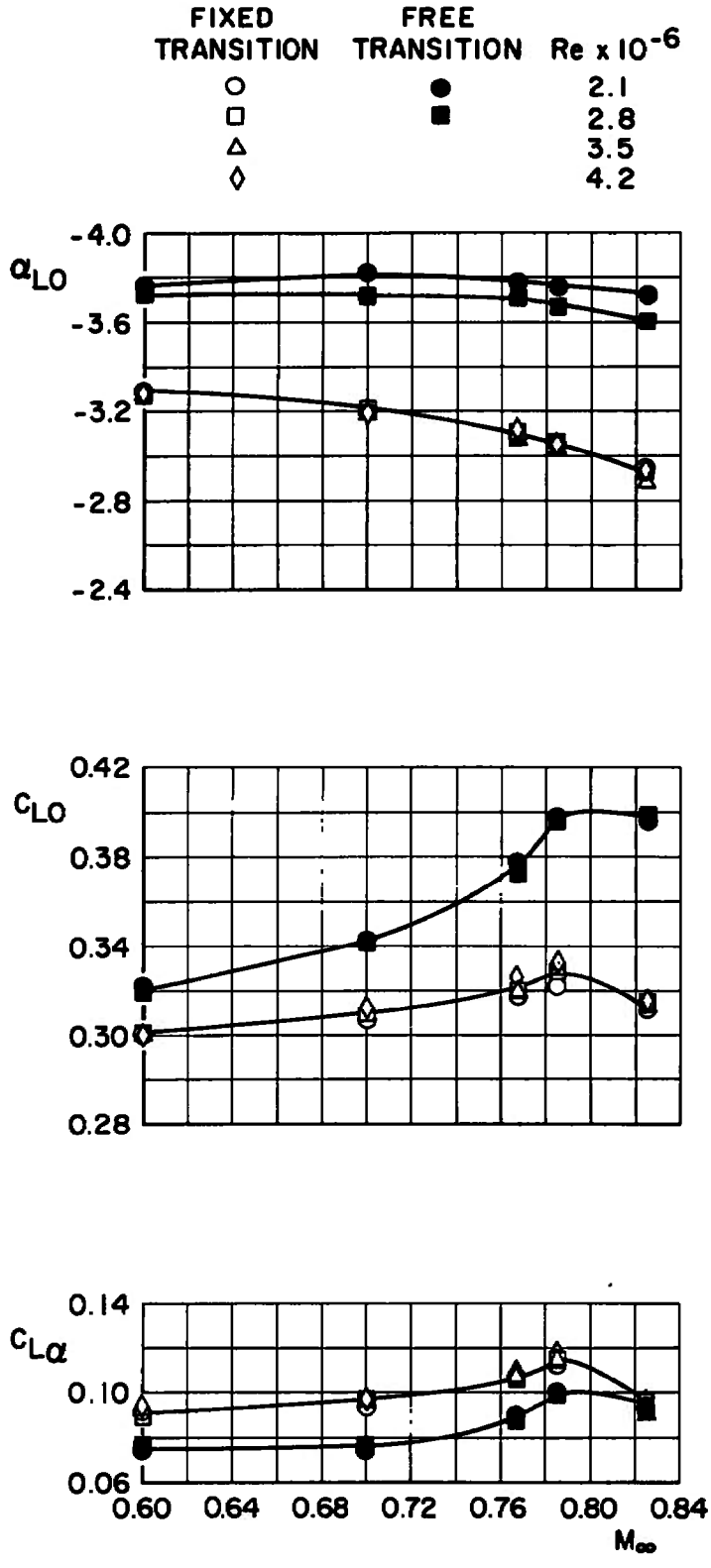

Fig. 10 Variation of α_{L_o}, C_{L_o}, and C_{L_α} with Mach Number for the Wing-Fuselage Configuration

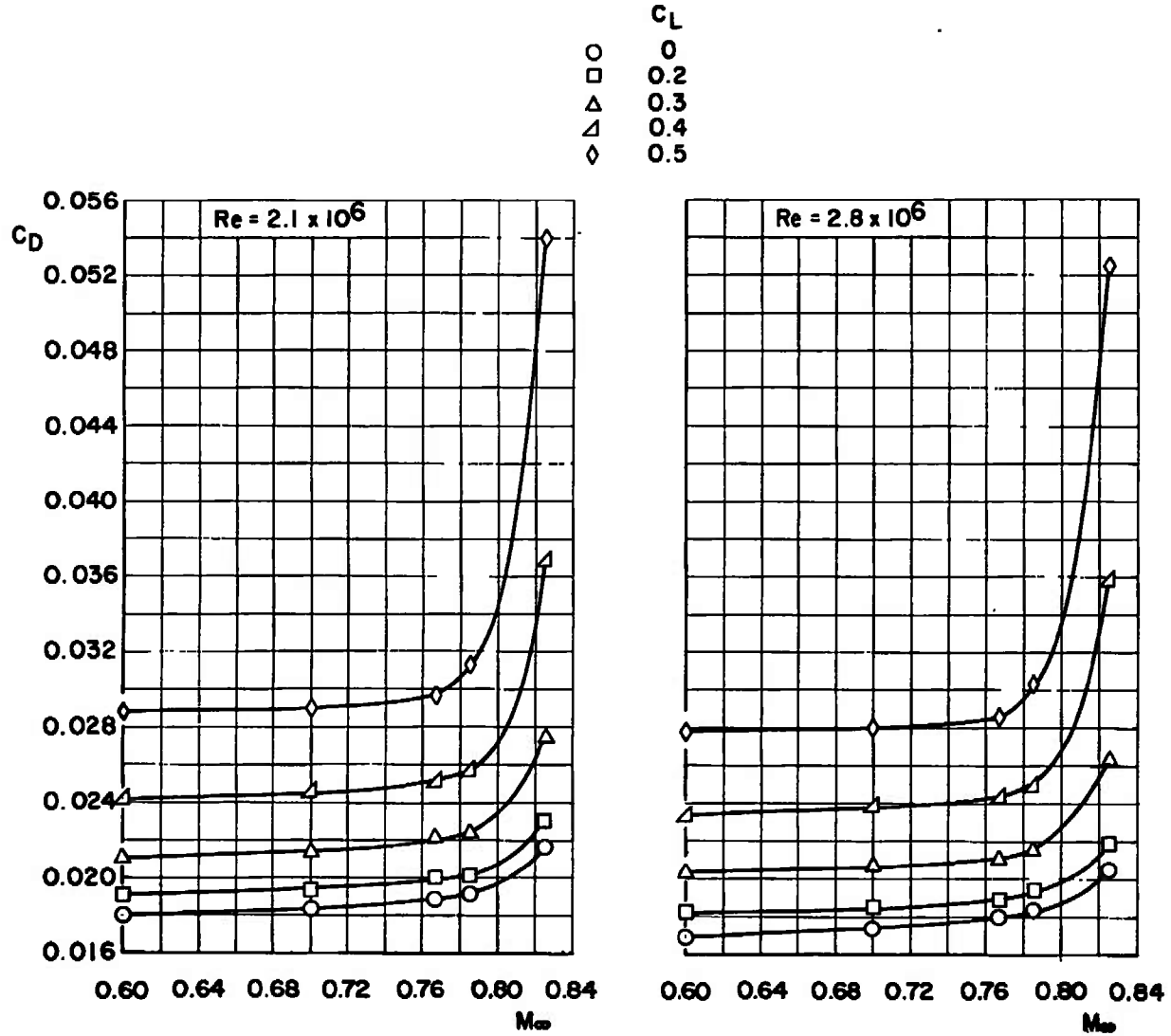

a. Fixed Transition

Fig. 11 Variation of C_D with Mach Number for the Wing-Fuselage Configuration

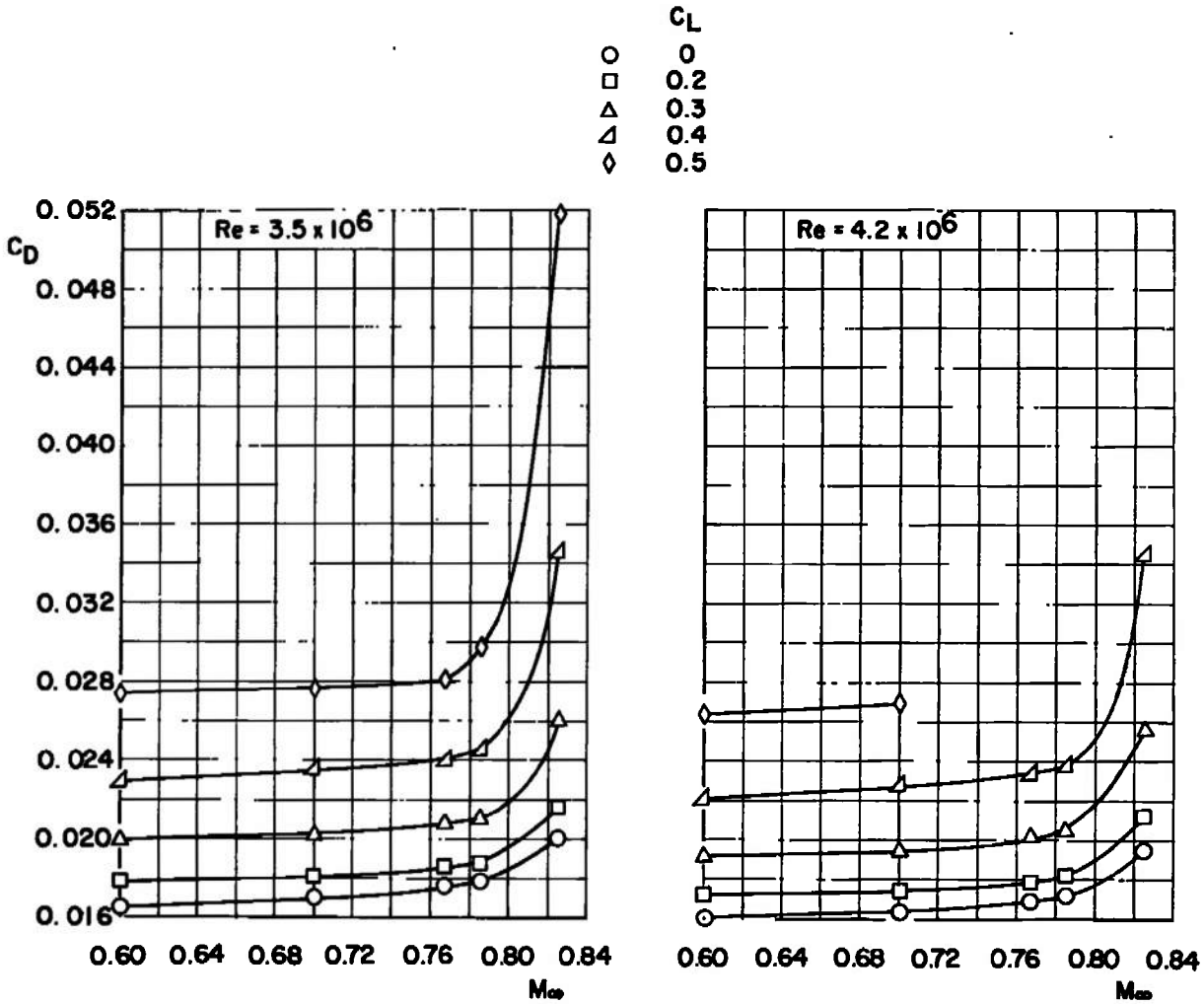

a. Concluded
Fig. 11 Continued

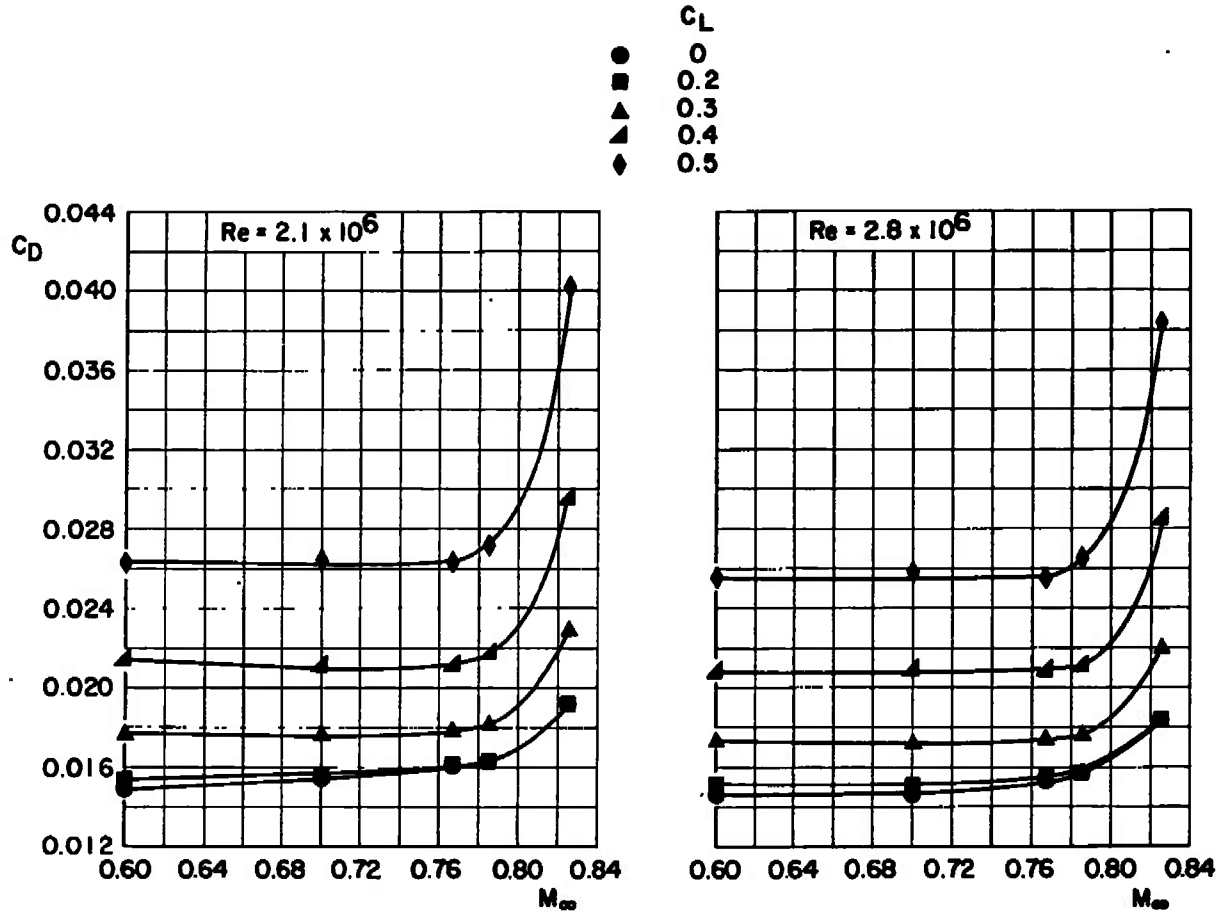

b. Free Transition
Fig. 11 Concluded

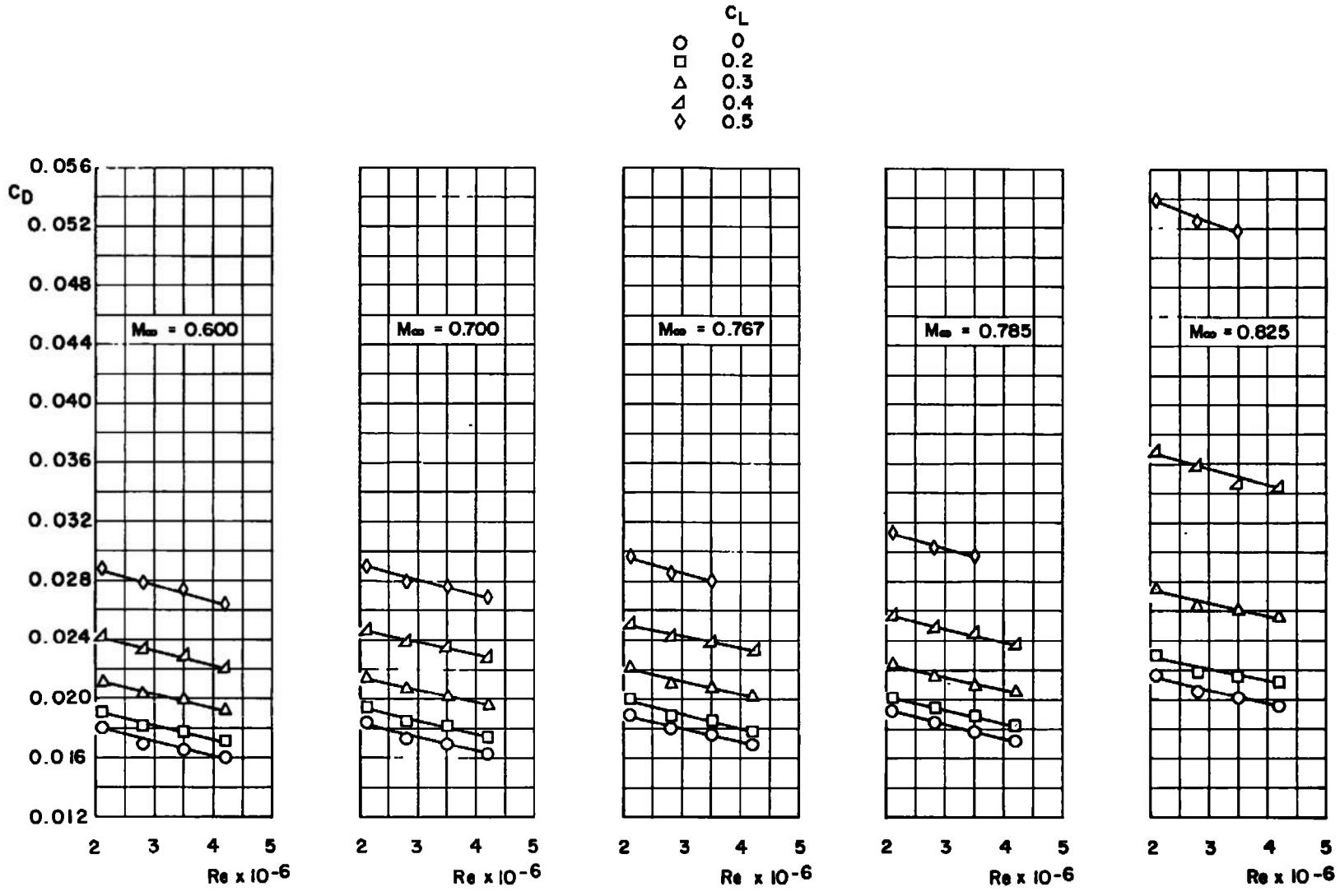

Fig. 12 Variation of C_D with Reynolds Number for the Wing-Fuselage Configuration, Fixed Transition

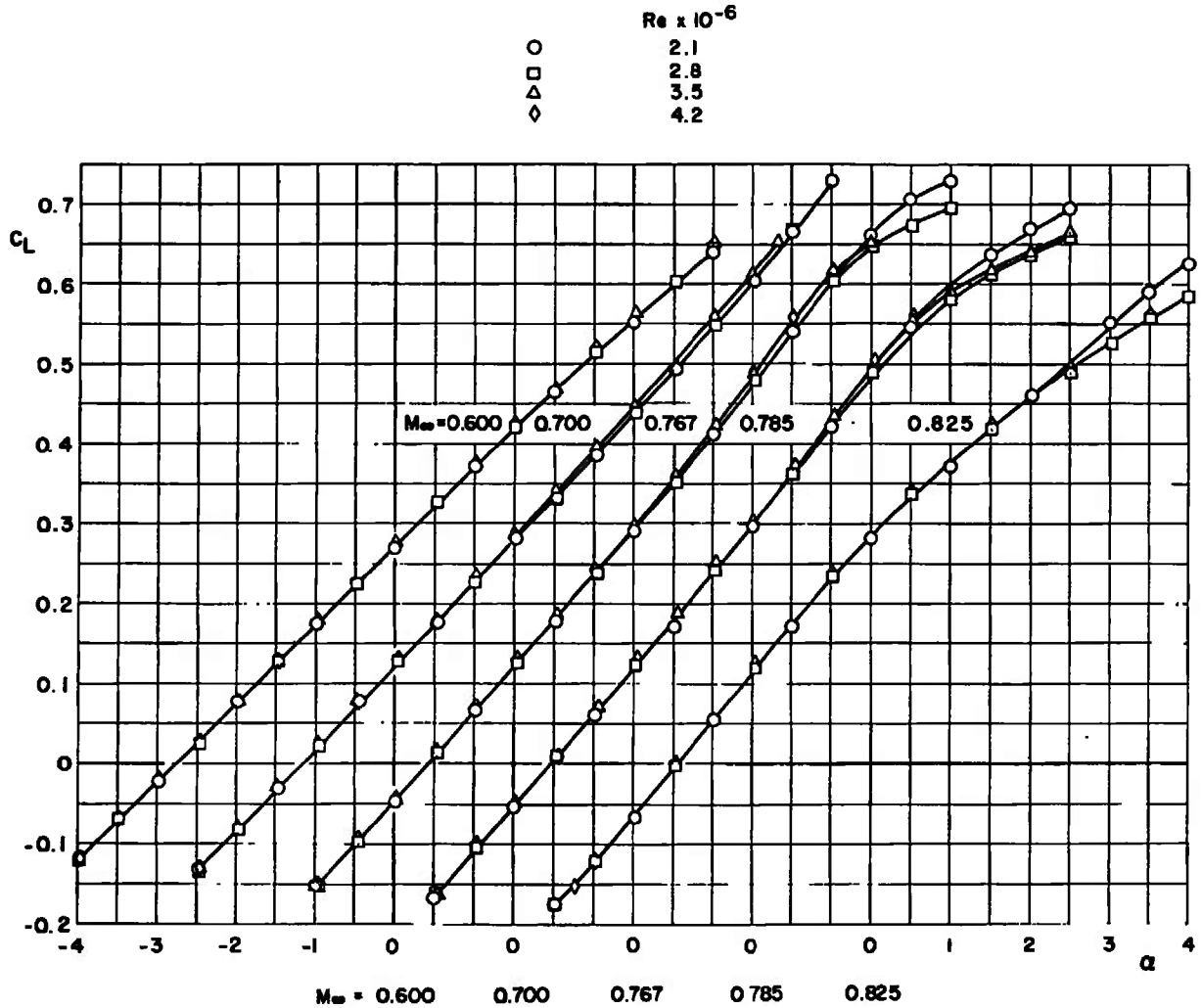

a. C_L

Fig. 13 Effects of Reynolds Number Variation on the Aerodynamic Coefficients of the Wing-Fuselage-Tail Configuration at Mach Numbers from 0.600 to 0.825

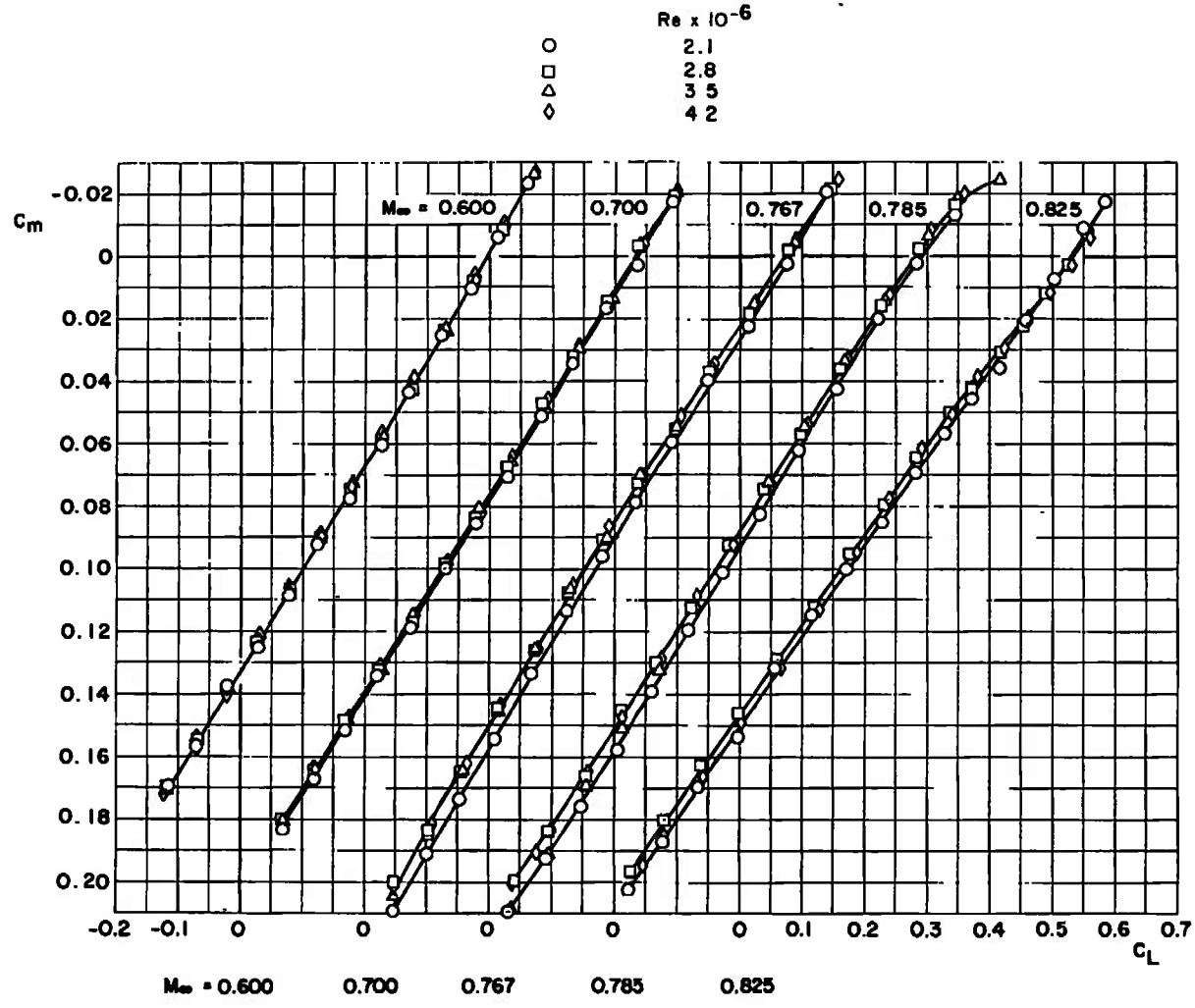

b. C_m

Fig. 13 Continued

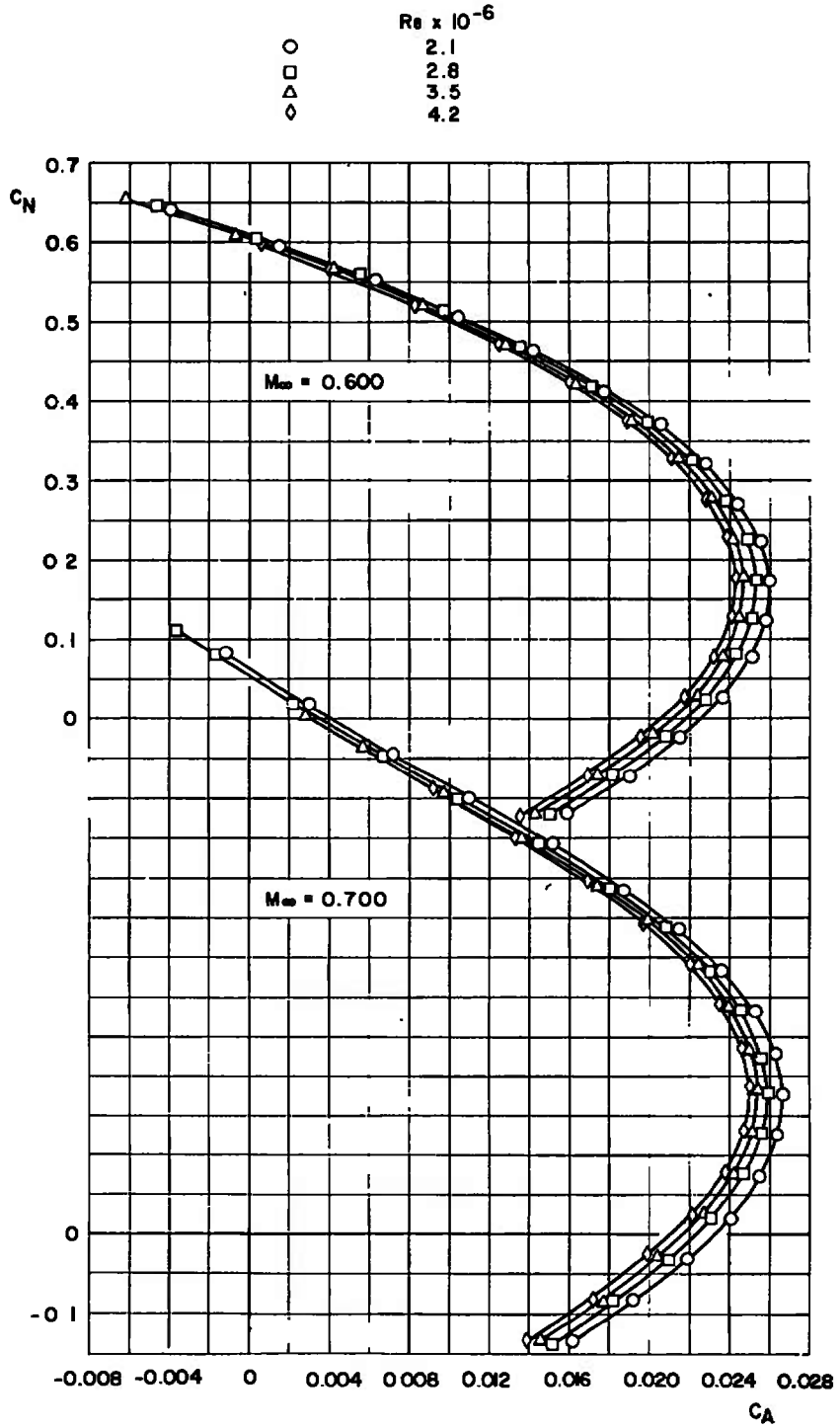

c. C_A

Fig. 13 Continued

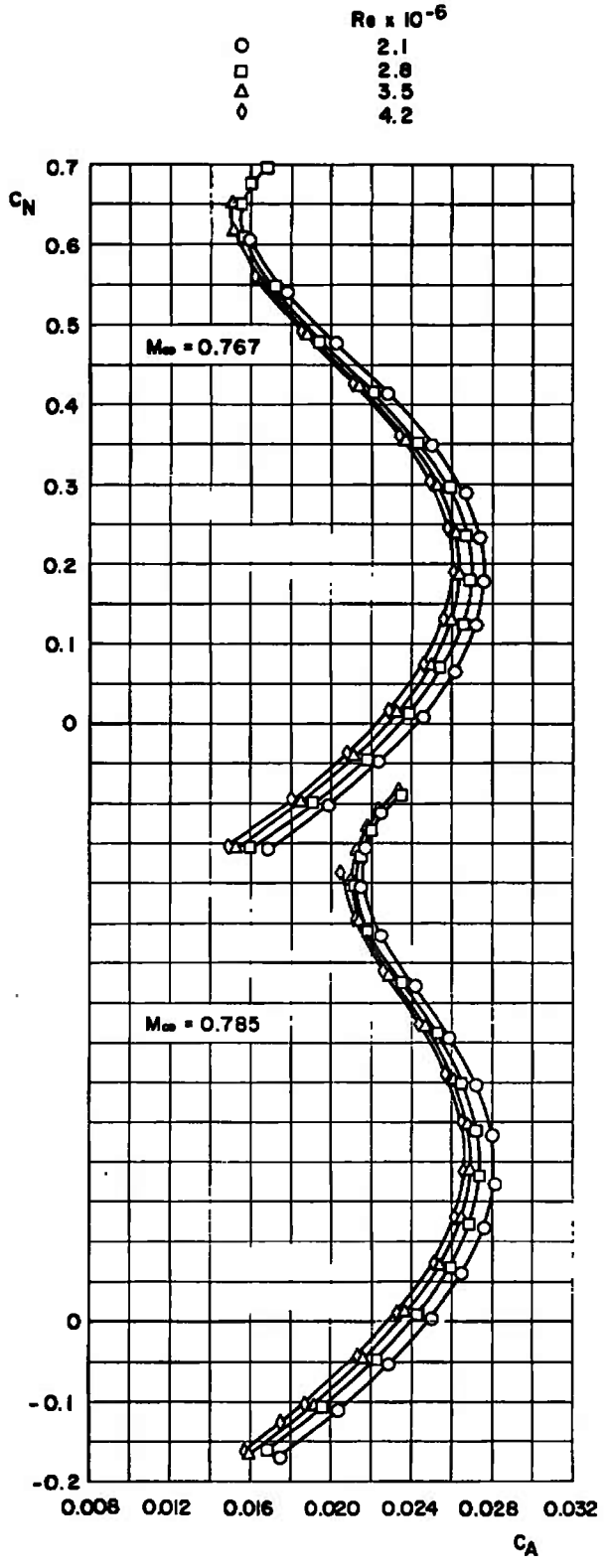

c. Continued

Fig. 13 Continued

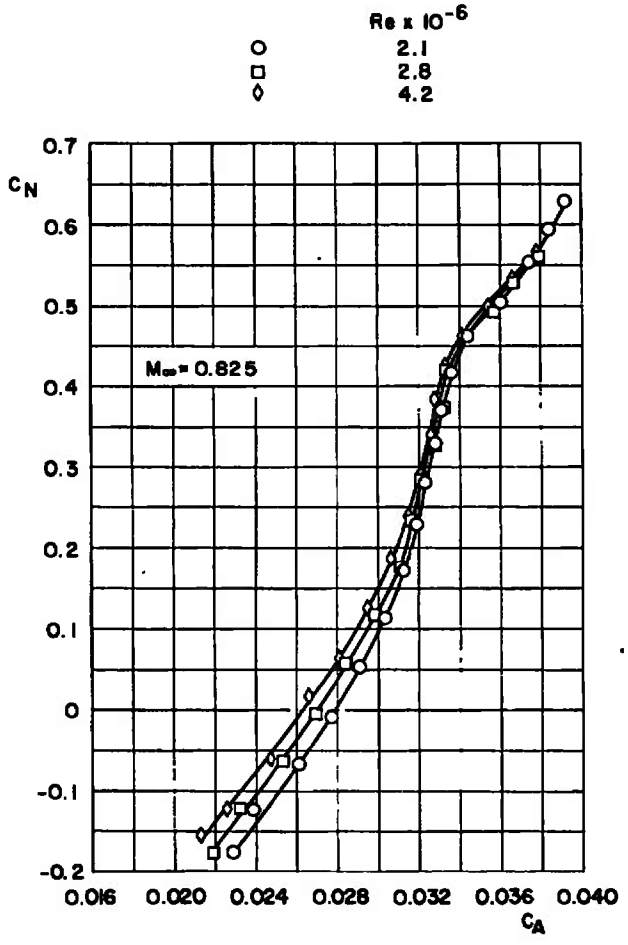

c. Concluded
Fig. 13 Continued

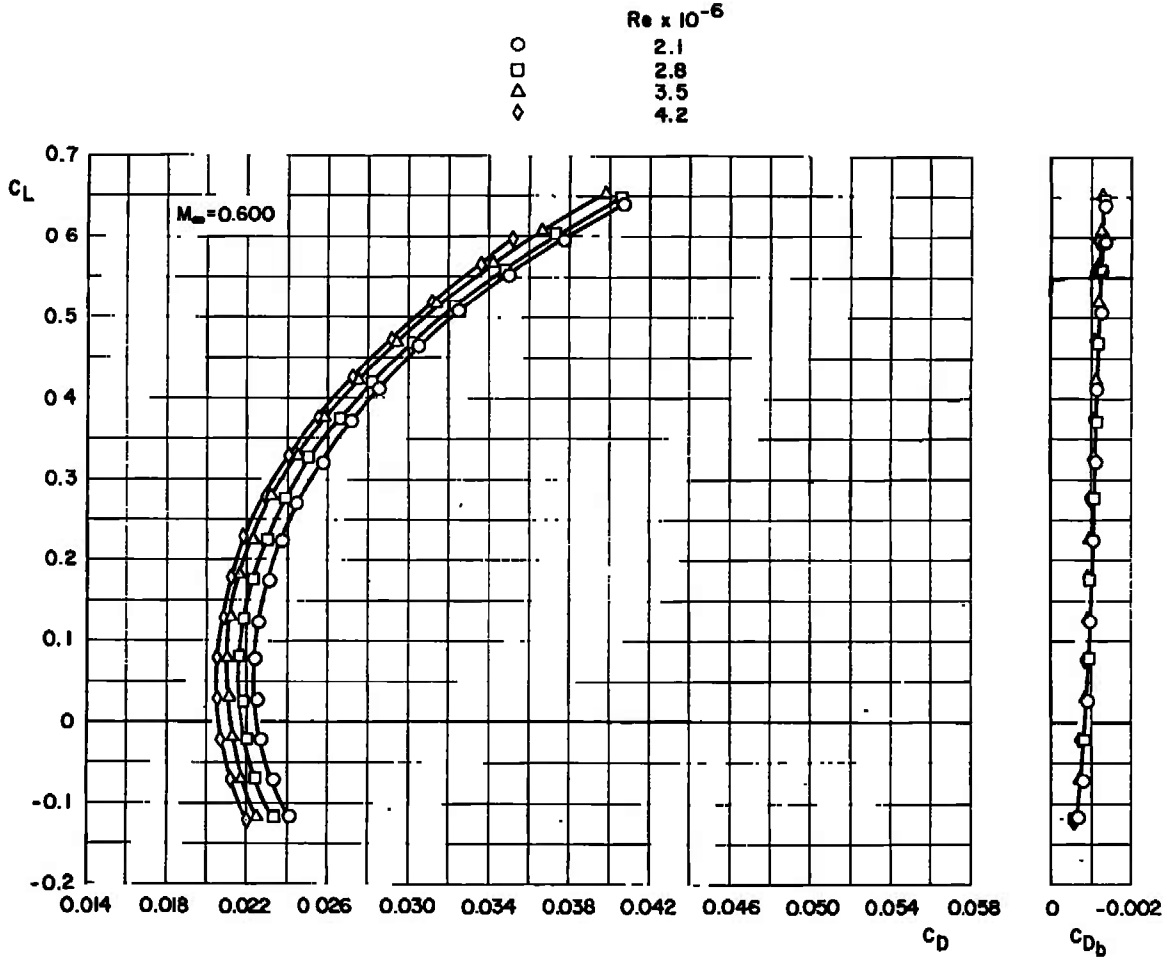

d. C_D and C_{D_b}
Fig. 13 Continued

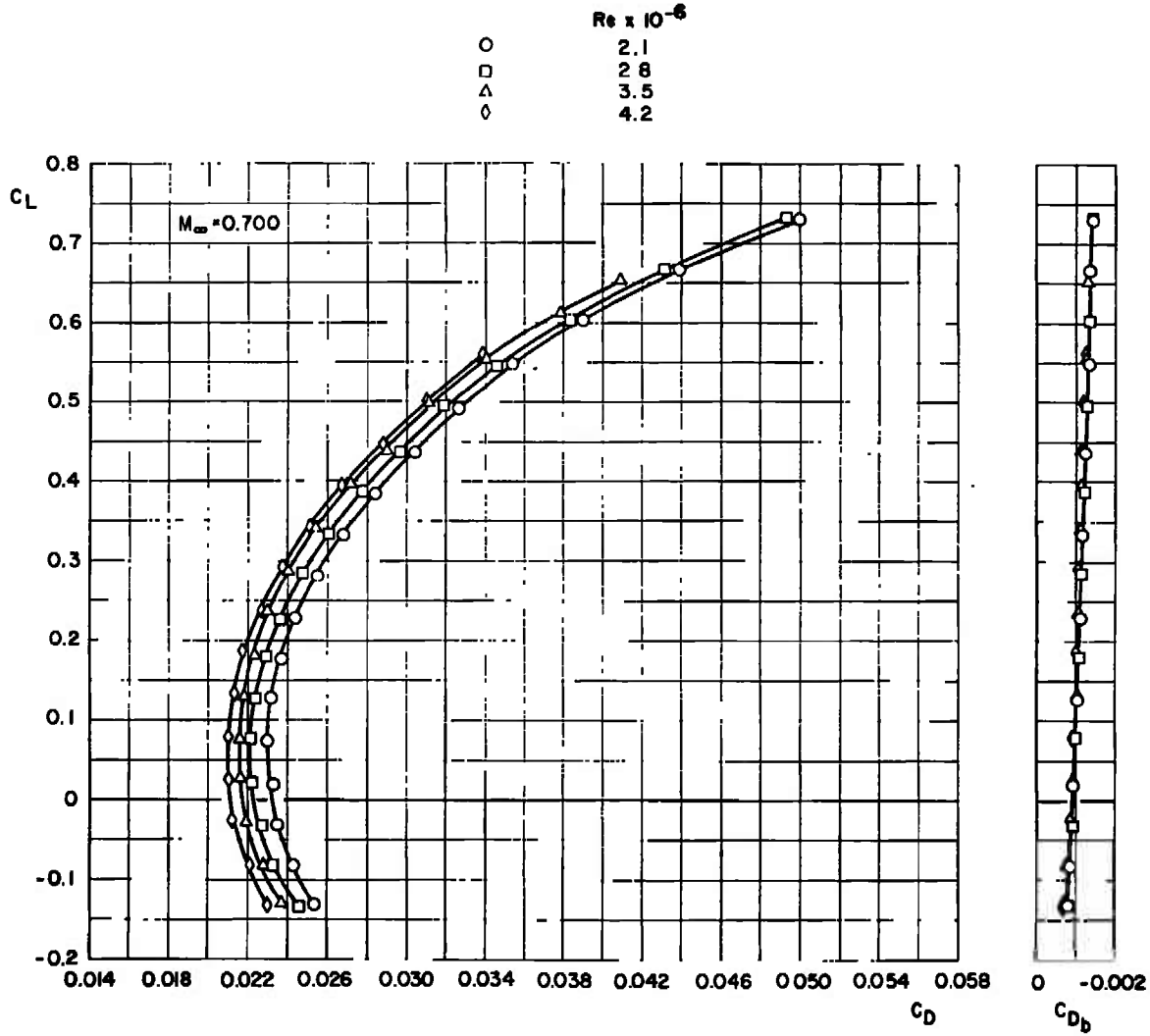

d. Continued

Fig. 13 Continued

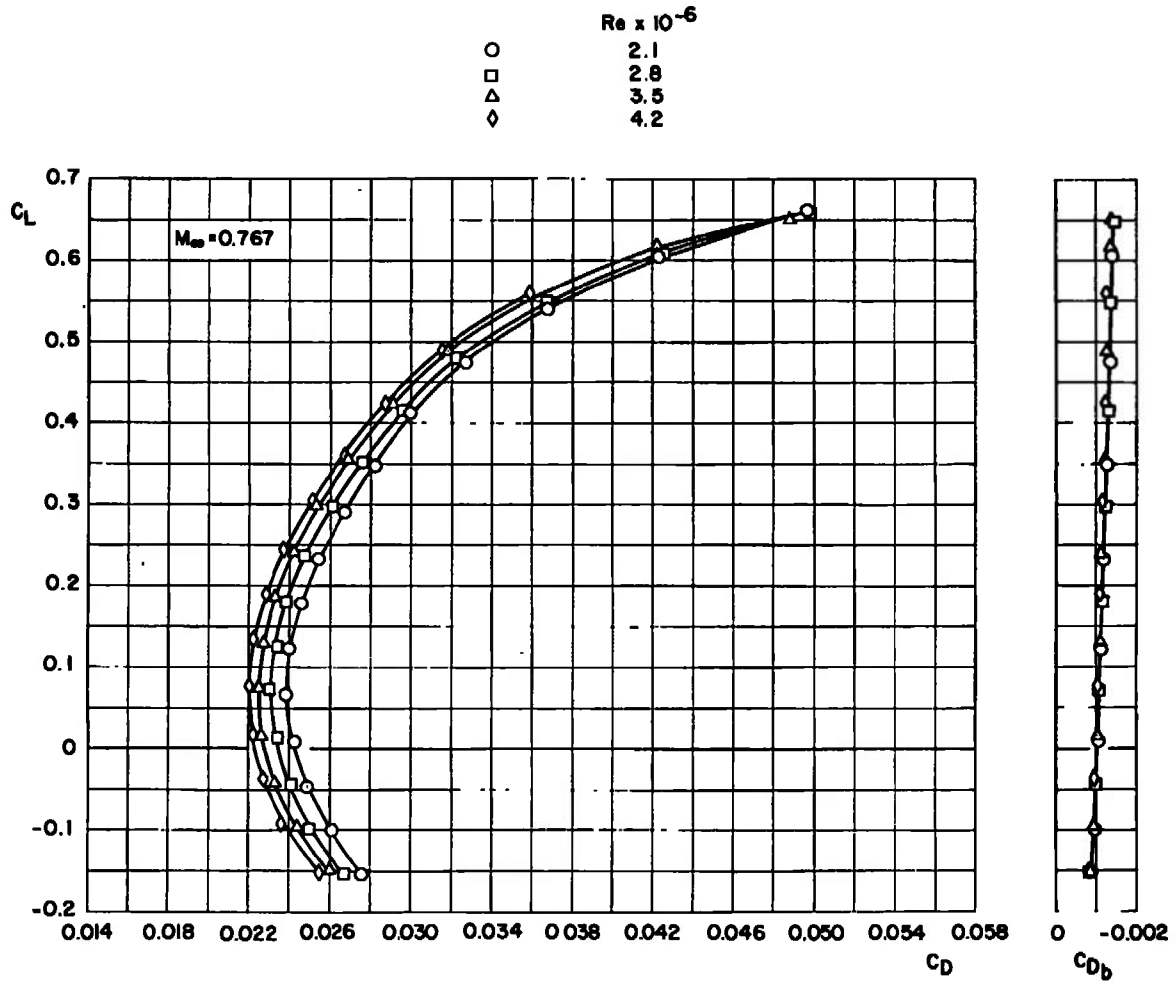

d. Continued

Fig. 13 Continued

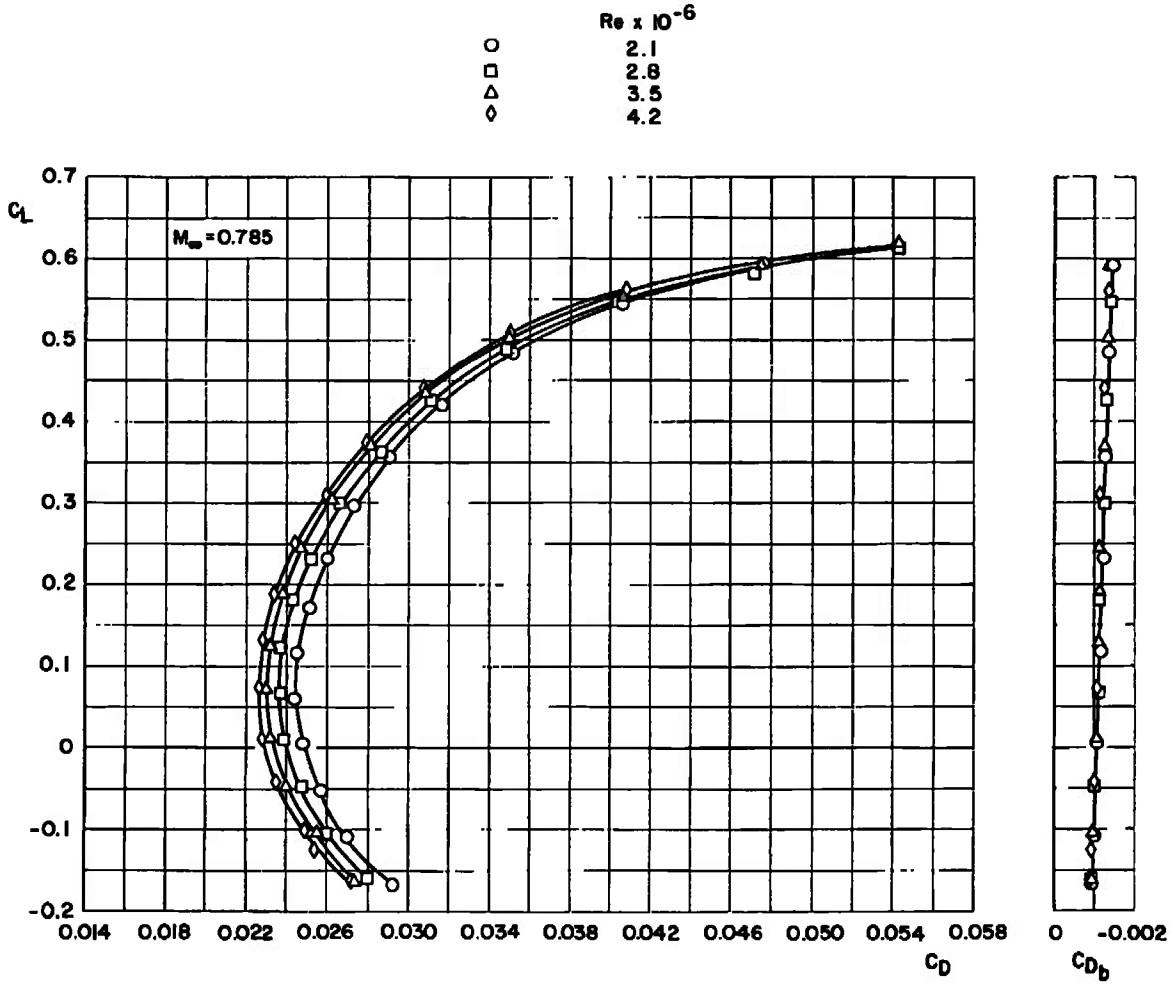

d. Continued

Fig. 13 Continued

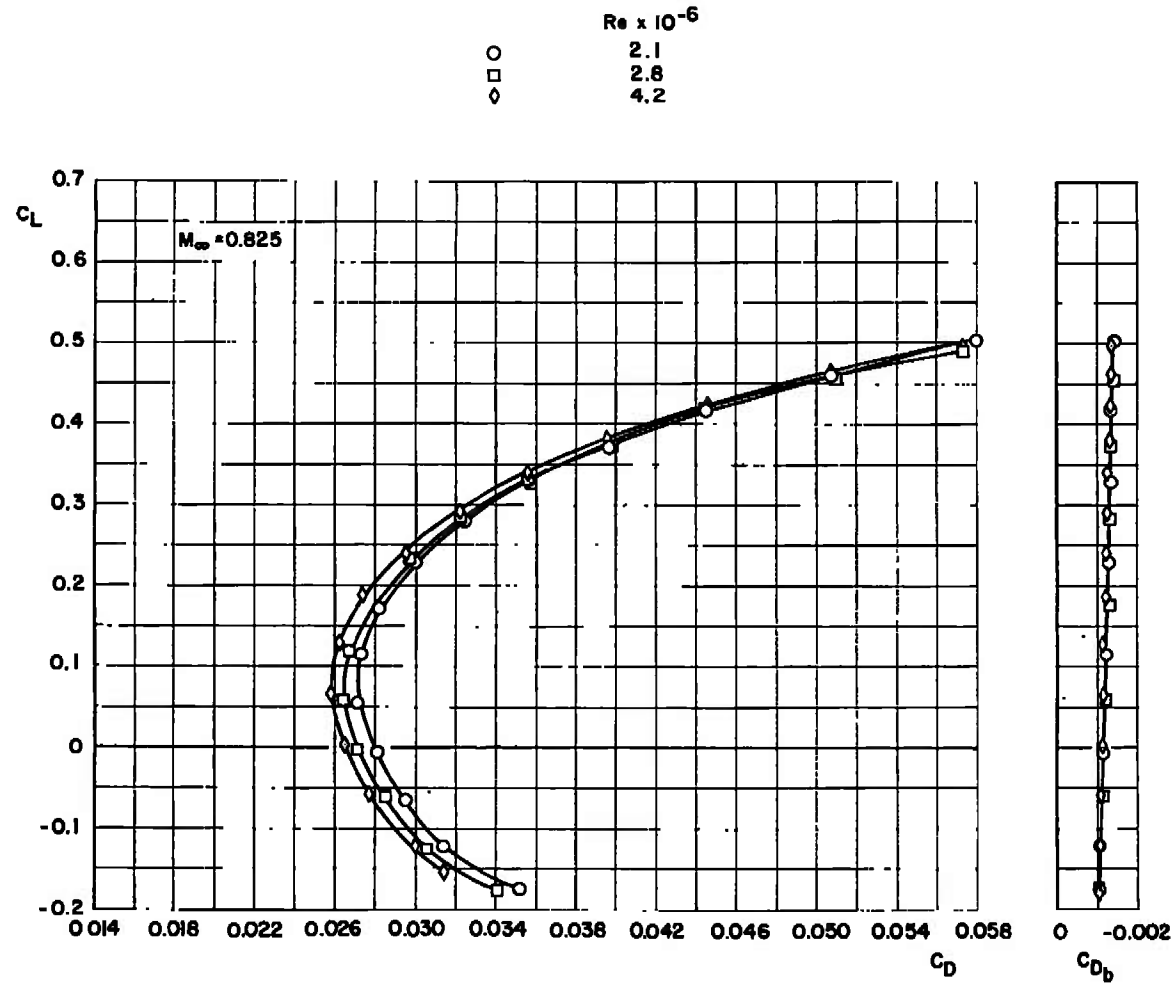

d. Concluded

Fig. 13 Concluded

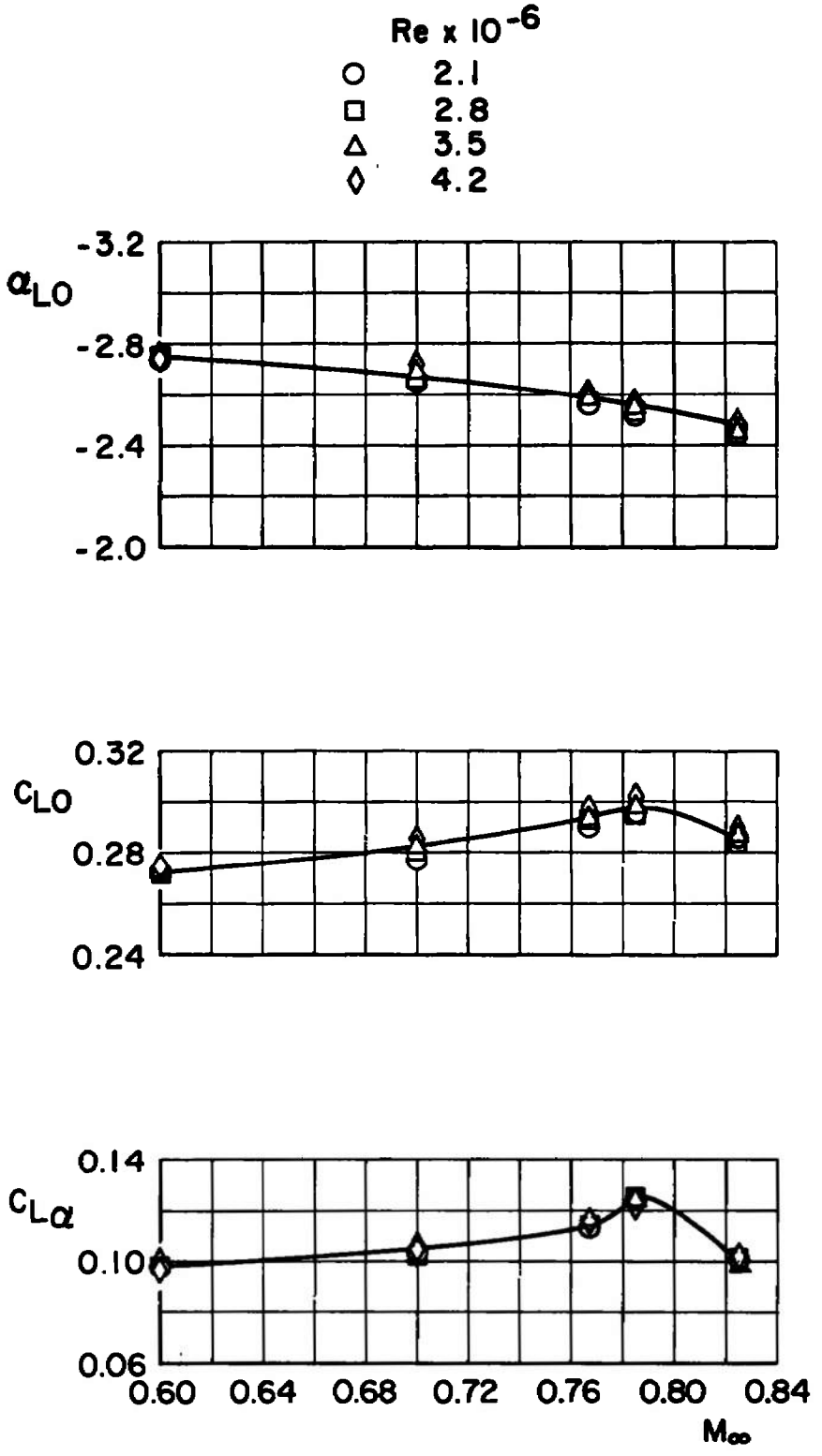

Fig. 14 Variation of α_{L_0}, C_{L_0}, and C_{L_α} with Mach Number for the Wing-Fuselage-Tail Configuration

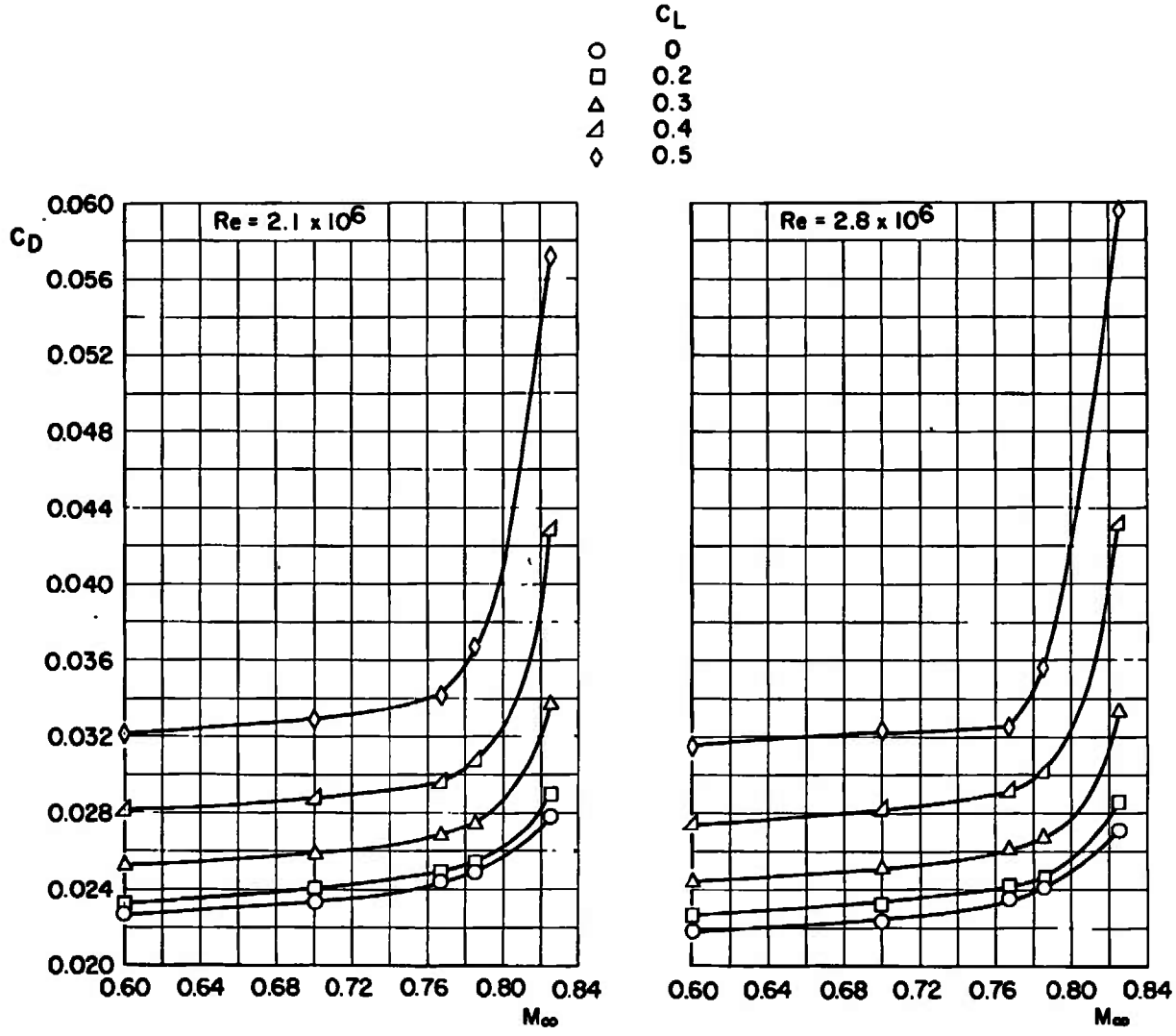

Fig. 15 Variation of C_D with Mach Number for the Wing-Fuselage-Tail Configuration

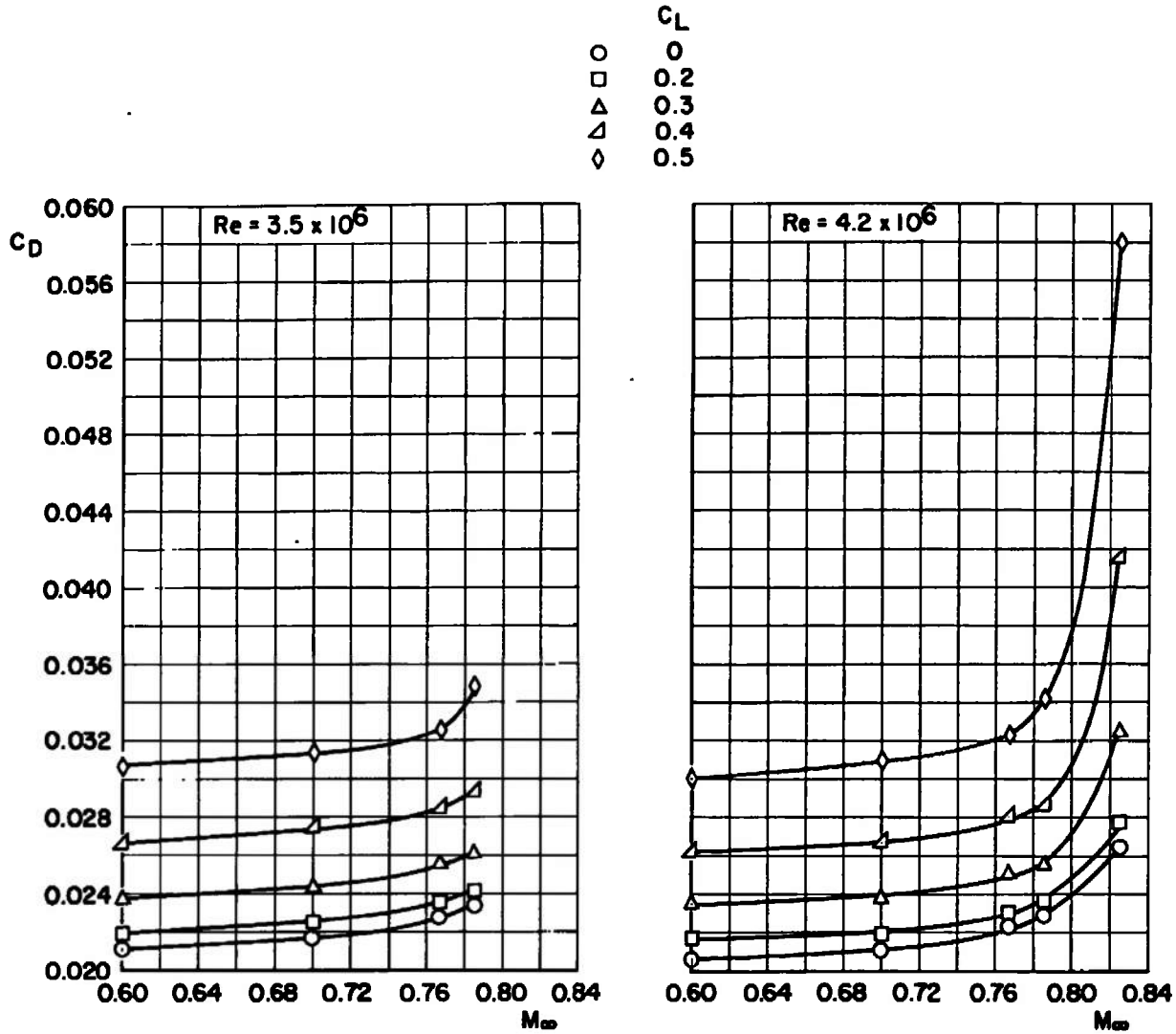

Fig. 15 Concluded

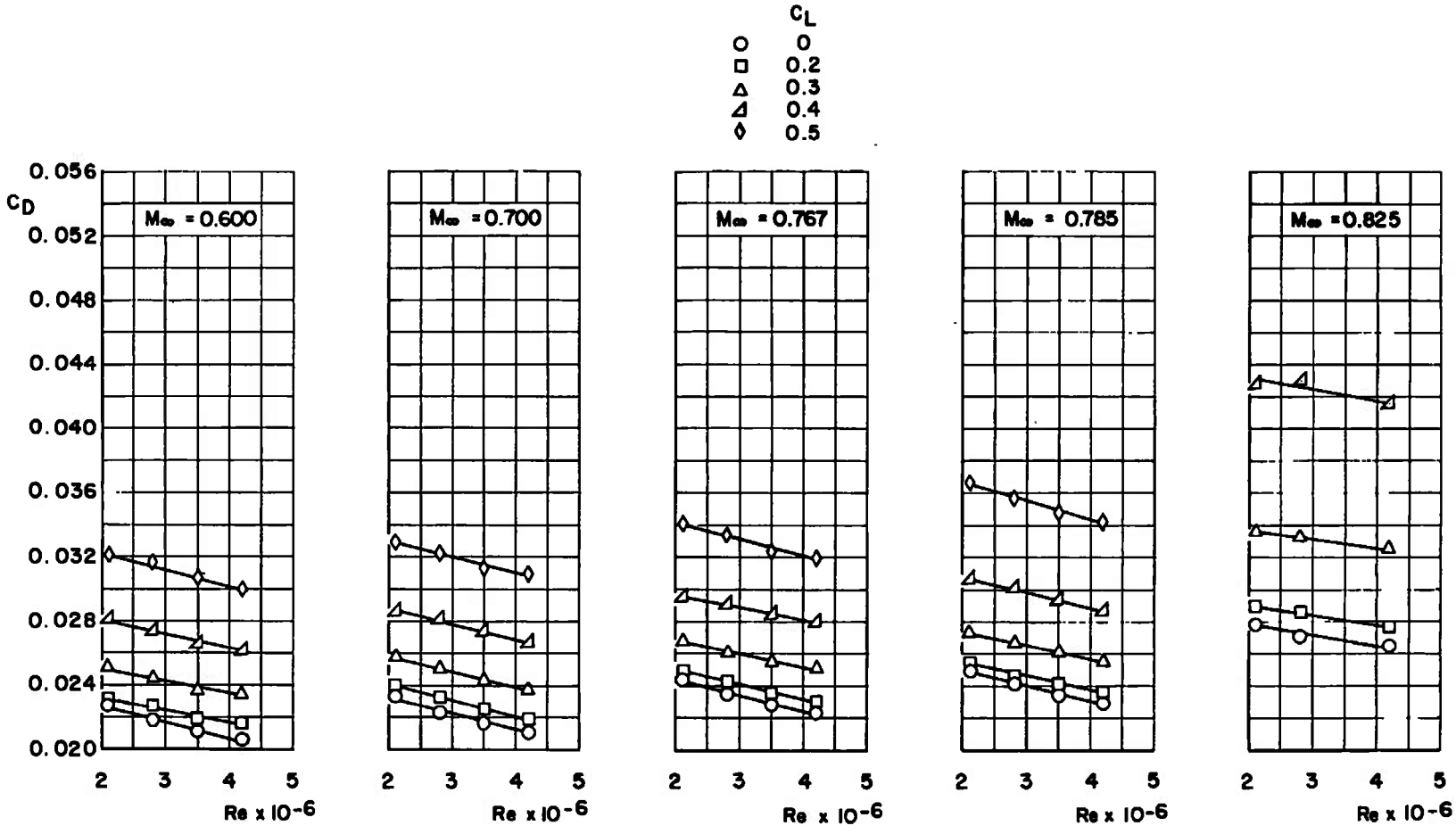

Fig. 16 Variation of C_D with Reynolds Number for the Wing-Fuselage-Tail Configuration, Fixed Transition

DOCUMENT CONTROL DATA - R & D

(Security classification of title, body of abstract and indexing annotation must be entered when the overall report is classified)

1 ORIGINATING ACTIVITY (Corporate author)	2a. REPORT SECURITY CLASSIFICATION
Arnold Engineering Development Center ARO, Inc., Operating Contractor Arnold Air Force Station, Tennessee 37389	UNCLASSIFIED
	2b. GROUP N/A

3 REPORT TITLE

TESTS CONDUCTED IN THE AEDC 16-FT TRANSONIC TUNNEL ON A 0.0226-SCALE MODEL OF THE C-5A AIRCRAFT FOR DATA CORRELATION BETWEEN THREE TRANSONIC WIND TUNNELS

4 DESCRIPTIVE NOTES *(Type of report and inclusive dates)*

Final Report - December 30, 1969 to January 20, 1970

5. AUTHOR(S) *(First name, middle initial, last name)*

J. A. Black, ARO, Inc.

6 REPORT DATE	7a. TOTAL NO. OF PAGES	7b. NO. OF REFS
July 1971	60	5

8a. CONTRACT OR GRANT NO.	9a. ORIGINATOR'S REPORT NUMBER(S)
F40600-72-C-0003 b. PROJECT NO. 1366 c. Program Element 62201F d.	AEDC-TR-71-105
	9b. OTHER REPORT NO(S) *(Any other numbers that may be assigned this report)* ARO-PWT-TR-71-68

10 DISTRIBUTION STATEMENT

Approved for public release; distribution unlimited.

11 SUPPLEMENTARY NOTES	12 SPONSORING MILITARY ACTIVITY
Available in DDC	Aeronautical Systems Division (YAT) Wright-Patterson AFB, Ohio 45433

13. ABSTRACT

Tests were conducted in the Propulsion Wind Tunnel (16T) on two configurations of a 0.0226-scale model of the C-5A aircraft for the purpose of data correlation with other major transonic test facilities. The results reported herein were obtained at Mach numbers from 0.600 to 0.825 and Reynolds numbers from 2.1 million to 4.2 million and represent the AEDC contribution to the correlation study.

DD FORM 1 NOV 65 1473

14. KEY WORDS	LINK A		LINK B		LINK C	
	ROLE	WT	ROLE	WT	ROLE	WT
C-5A						
transonic wind tunnels						
test facilities						
correlation						